

SHALY SANDSTONE LOG ANALYSIS:
CONVENTIONAL AND SPREADSHEET OPTIMIZATION PROCEDURES

by

John H. Doveton

Kansas Geological Survey
Open-file Report 99-52

Disclaimer

The Kansas Geological Survey does not guarantee this document to be free from errors or inaccuracies and disclaims any responsibility or liability for interpretations based on data used in the production of this document or decisions based thereon. This report is intended to make results of research available at the earliest possible date, but is not intended to constitute final or formal publication.

Kansas Geological Survey
1930 Constant Avenue
University of Kansas
Lawrence, KS 66047-3726

**Shaly sandstone log analysis: Conventional
and Spreadsheet Optimization procedures**

By John H. Doveton

1999

LOG ANALYSIS MODELS FOR SHALY SANDSTONES

The problem of shale contamination is particularly important in the reservoir evaluation of shaly sandstones, and its neglect can lead to significant errors in both porosity and hydrocarbon saturation evaluations. The responses of the logging tools that have been reviewed are affected to some degree by the proportion of the shale and, to a lesser extent, its distribution.

Log analysts generally distinguish three distribution types of shale:

(1) *Laminar shale*

This consists of thin laminations of shale which separate stringers or beds of clean sandstone. The occurrence of these laminations is not accompanied by a reduction in the porosities of the sandstone stringers themselves, but there is an overall reduction of the bulk porosity of the total rock.

(2) *Structural shale*

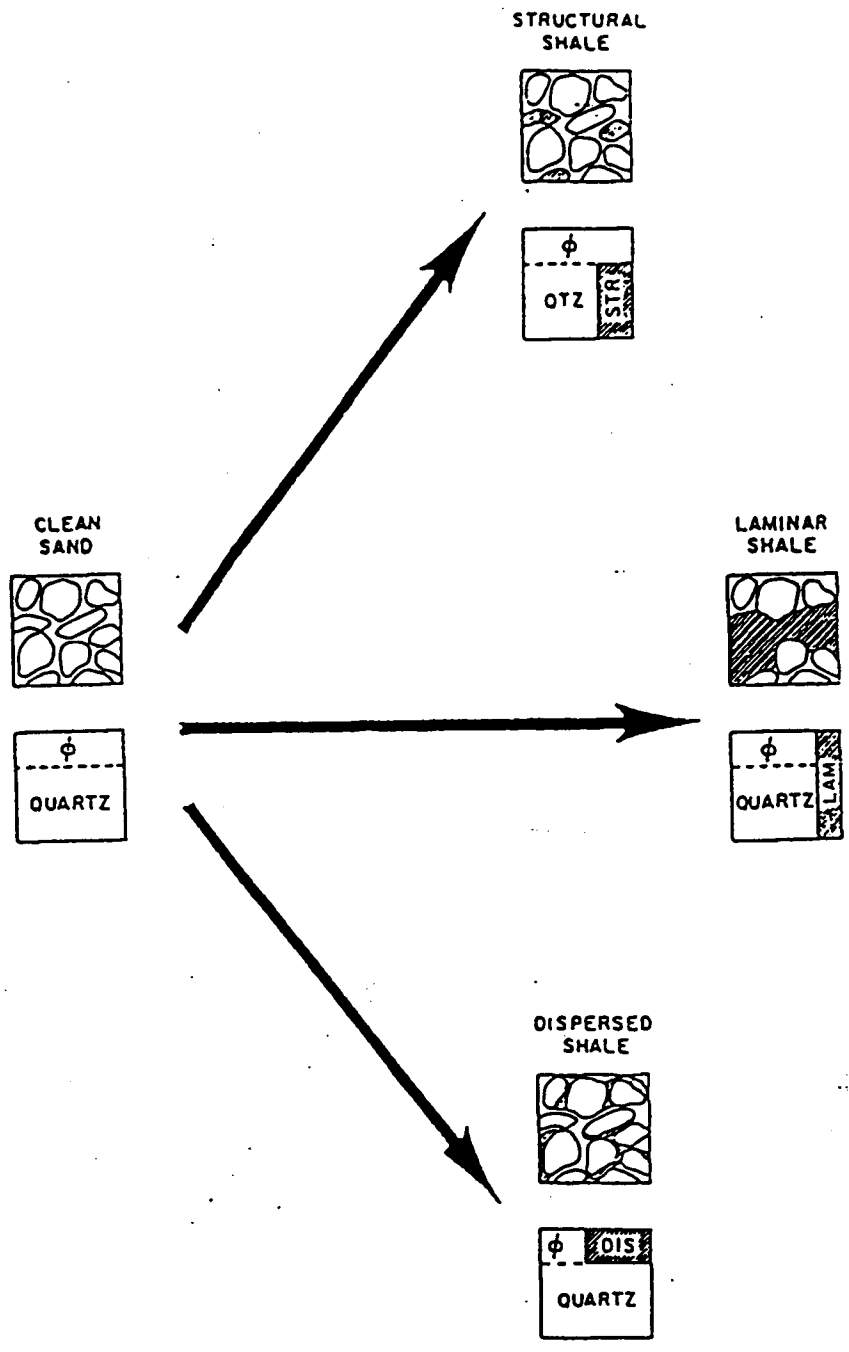
The term describes sandstones in which some of the grains of the framework are shale fragments, diagenetically altered minerals, etc. A transition from a clean orthoquartzite is not necessarily matched by any reduction in porosity.

(3) *Dispersed shale*

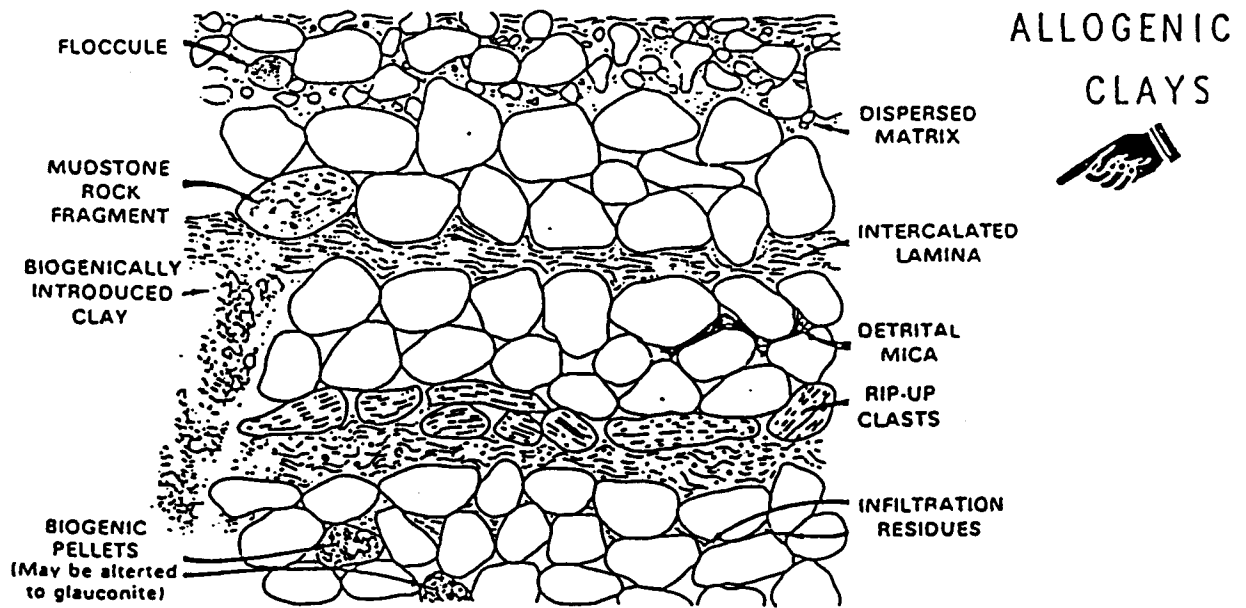
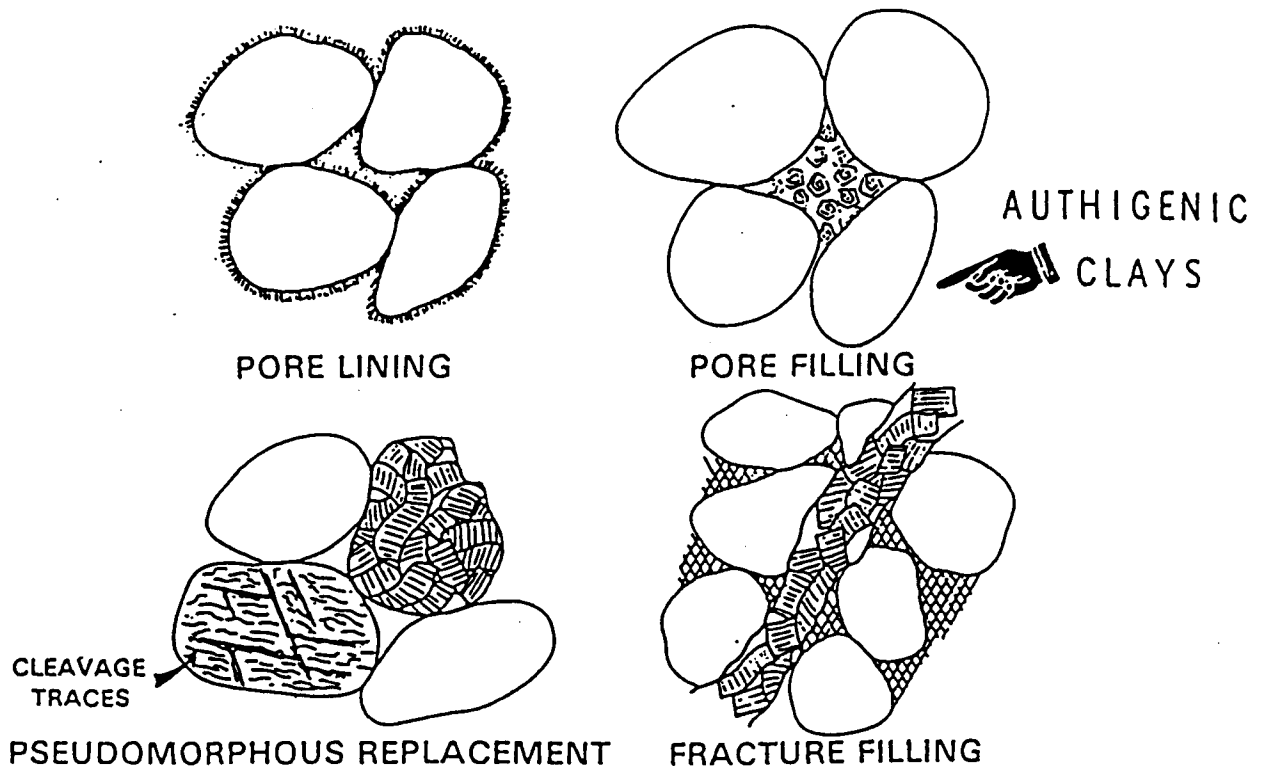
Dispersed shale consists of pore-filling clay minerals whose development leads to a progressive reduction in porosity.

These three shale distribution types form natural endmembers of ranges of variation from a theoretical pure orthoquartzite to more shaly counterparts as is demonstrated by the diagram on the next page. The basis for description by log analysts is *morphology* - the geometrical manner in which the shale is distributed through the rock; the geological description is keyed to *genesis* - the process that was the origin of the shale. Although the log analysis terminology may be unfamiliar to many geologists, it is easy to assign different categories of authigenic and allogenic clay morphologies among the shale distribution types. In practice, the range of variation between clean and shaly sands most commonly follows a trend which corresponds to a mixture of dispersed and laminar shale. This characterization is possible by a crossplot of neutron and density logs and is reviewed in a later section.

Up until the 1960's, shaly sandstones received much more attention from log analysts than geologists, who tended to regard clay minerals in most sandstones to have minor occurrence. This perception was caused partly by the methods that geologists used to observe sandstones. Pore-lining clay minerals are not obvious on thin-sections of sandstones, while the sieving of disaggregated sandstones relegated clay minerals to the neglected fraction of 'fines'. The introduction of the scanning electron microscope caused a radical change of viewpoint, when the pore networks of many sandstones were seen to be lined profusely with clay minerals.



Distribution types of shale in shaly sandstones as hypothetical limiting cases of a simple model for log analysis (after Schlumberger publications).



Modes of occurrence of authigenic and allogenic clays in sandstones (from Wilson and Pittman, 1977).

Shale indicators: estimation of the volumetric proportion of shale

A variety of indicators are used from various logs in the assessment of the proportion of shale in a zone. Most of them follow the same methodology of establishing a value for a clean zone, locating a value that best typifies shales within the interval of interest, and interpolating between these two extremes. The more commonly used shale indicators are the SP log, gamma ray log, and neutron-density log combination.

The SP log

In shaly, permeable formations, the displacement of the potential from the shale reading is reduced to a pseudo-static potential (PSP). The relationship between PSP and SSP is approximately a function of shale content which is generally quantified as:

$$\alpha = \text{PSP/SSP}$$

The quantity $(1 - \alpha)$ has been used for many years as an estimate of the proportional shale content. However, laboratory and lab work by Griffiths (1952) showed that the relationship between α and shale content was by no means linear: calculations based on a would generally provide marked overestimations of shale content.

Gamma ray log

In using a gamma ray log, first a 'shale base line' must be found as the reading for 'normal shales' (as distinct from uranium-rich 'hot shales') in the stratigraphic sequence. Then a 'clean formation line' is located to represent zero shale and should coincide with the lower readings that occur in clean units of interest. Then the volumetric proportion of shale, V_{sh} , of a zone is estimated by interpolating the zone log reading, L , between the extremes of a log reading of a "clean" (shale-free) formation, C , and the reading of a typical shale, S . The equation is then:

$$V_{sh} = \frac{L - C}{S - C}$$

This estimate is often known as the "gamma-ray index" (GRI) and represents the proportion by weight of radioactive material calibrated to the reference shale. Some log analysts apply one of a variety of functions to estimate the volume of clay, V_{cl} . This relationship varies with the stratigraphic age and sedimentary facies of the shale. However, it has been reported in the literature (e.g. Yaalon, 1962) that the "average" shale contains approximately 60% clay minerals. Therefore, as a first approximation:

$$V_{cl} = 0.6 \cdot V_{sh}$$

as suggested by Bhuyan and Passey (1994). There appears to be a great deal of confusion regarding the distinction between 'shale' and 'clay' and the two terms are often used interchangeably by log analysts. As a general rule, it is better to stick with V_{sh} , particularly when using shale properties measured from logs to characterize equation parameters.

Use of the gamma-ray index interpolation assumes that the radioactive sources in the units evaluated, correspond to shale contents whose clay mineralogy and radioactive isotope composition is not markedly dissimilar from the bounding shales. If feldspars or micas occur in appreciable quantities, the assumption is invalidated. However, independent evaluation of other logs run in the same section often highlights the presence of additional disturbing components. Uranium mineralization can be major problem in some units, in which case it is better to use the computed gamma -ray (CGR) log, rather than the standard gamma-ray (SGR).

Neutron-density porosity logs

If two logs are used (most commonly the neutron and density logs) and are calibrated to the clean reservoir lithology, then the estimate is given by the equation:

$$V_{sh} = \frac{\phi_n - \phi_d}{\phi_{nsh} - \phi_{dsh}}$$

The analyst provides the boundary values from an inspection of the section itself because of the extreme variability of shale properties both laterally and with depth.

Multiple shale indicators

In sections which have been logged by a variety of tools, separate estimates of the shale content are computed for the shale indicators which are available. It is not uncommon for these estimates to differ from one another to varying degrees, and the lowest estimate is usually taken to be the most valid. This stipulation is made on the grounds that, if anything, a shale indicator will tend to overestimate the shale content. This is not an unreasonable thesis, since accessory components other than shale will generally result in an increased apparent shaliness as recorded by the logging tools.

Correction of porosities for shale effect

Simple calculations for porosity estimation from a single log assume that shale effects are not significant or that they can be disregarded. When shale effects are significant, the estimated porosities are apparent (Φ_a) and should be corrected to an effective porosity (Φ_e) through use of V_{sh} estimates and log properties of the shales in the sequence of interest. The correction for shale involves an expansion of the porosity estimation equations to:

$$\begin{aligned} \text{for density, } \rho_b &= \phi \cdot \rho_f + V_{sh} \cdot \rho_{sh} + (1 - V_{sh} - \phi) \rho_{ma} \\ \text{for sonic } \Delta t &= \phi \cdot \Delta t_f + V_{sh} \cdot \Delta t_{sh} + (1 - V_{sh} - \phi) \Delta t_{ma} \\ \text{and for neutron log, } \phi_n &= \phi + V_{sh} \cdot \phi_{nsh} \end{aligned}$$

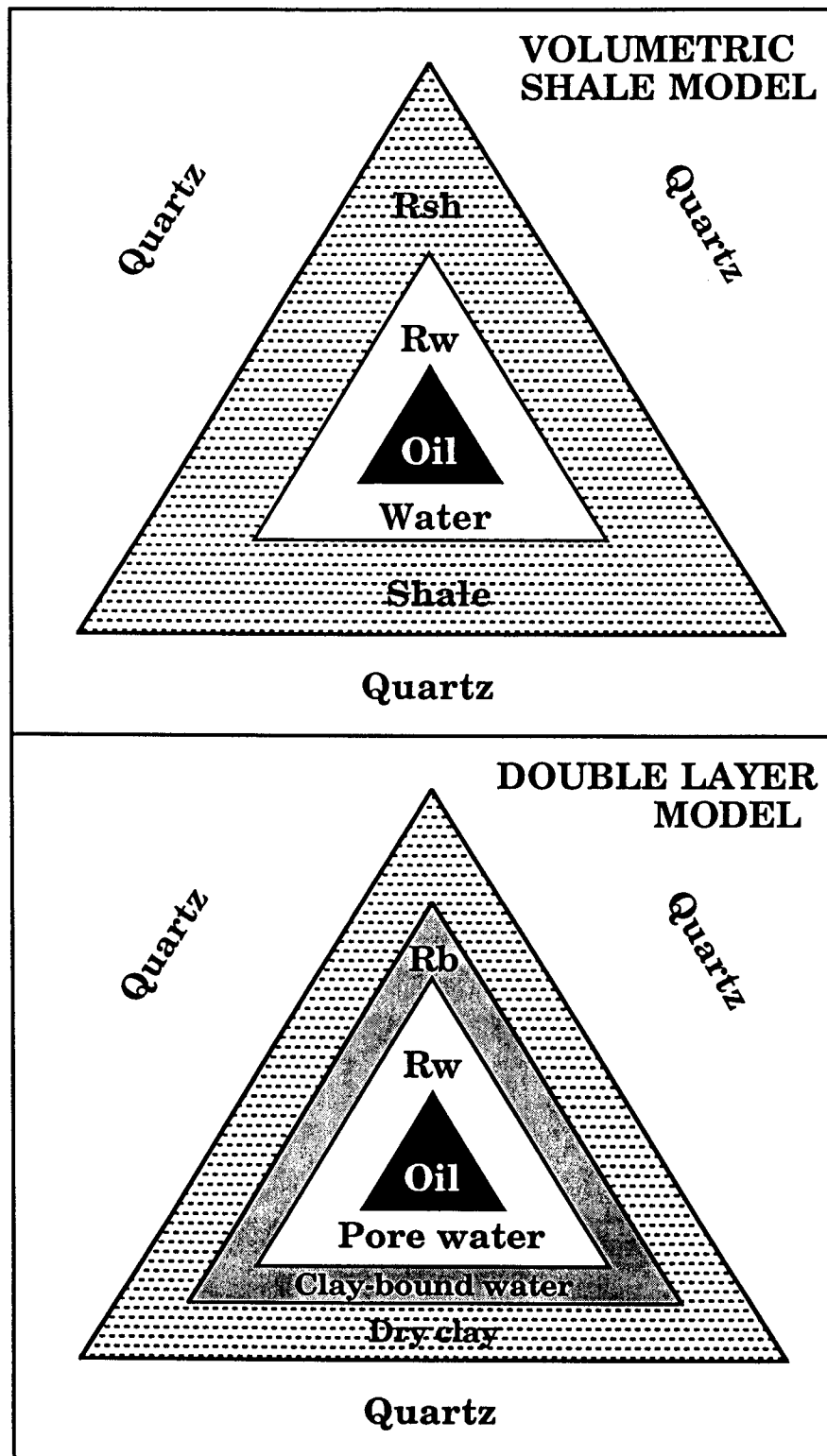
where Φ is the effective porosity, V_{sh} is the fraction of shale estimated from log(s) and ρ_{sh} , Δt_{sh} , and ϕ_{nsh} are readings of representative shales on the density, sonic, or neutron log.

Conductivity contributions of shales: the "shaly sandstone equation" computation of water saturation

Shales have moderately low resistivities, as can be seen on any resistivity log, and their presence as a component of shaly sandstones introduces a conductivity contribution that should be included together with the conductivity of the pore formation water in detailed reservoir analysis. As a general statement, if uncorrected resistivities are used in a conventional clean reservoir calculation of a shaly sand zone, the result will be an overestimation of water saturation, since the resistivities have been reduced below their true values by the conductivity of the shale component.

Two model families of shaly sandstone equations have been developed as expansions of the Archie equation to accommodate the conductivity effects of clay minerals and compute more accurate water saturations (Worthington, 1985). The older model considered the shale as a homogeneous conductive medium and developed resistivity equations keyed to V_{sh} , the volumetric fraction of shale in the rock. Although the physical basis of the model is incorrect, the equations often provide reasonable approximate solutions to water saturation, especially when the equation parameters are adjusted so that the results conform with local water saturation data measured from cores or production tests. Some of these equations are still widely used for this reason and also because of their relative simplicity and limited demands on additional input parameters.

The second, and more recent, model is based on the ionic double-layer observed in shaly sandstones. In reality, the conductivity of the shale component is a function of cation exchange capacities of the various types and abundances of clay minerals which are present. Since the cations are exchanged primarily at broken bonds on the edges of flakes or by lattice substitutions on cleavage surfaces, the phenomenon tends to be surface-area dependent rather than controlled simply by the volume of clay minerals. This implies that a fine grained clay has a higher exchange capacity than a coarser grained form of the same clay volume, and this observation is confirmed by experimental data. Since all the shale indicators estimate (at best) the volume of the shale component, no explicit assessment is made of the grain size or clay mineralogical variation. Although these factors are widely known among log analysts, it is difficult to design log analysis procedures to accommodate them, in the absence of a tool that measures cation exchange capacity directly. Consequently, the model equations that use cation-exchange data have been modified to variants that substitute quantities that can be measured on logs as surrogate variables.



The two major types of shaly sandstone model: Volumetric Shale and Double Layer (using the terminology of Worthington, 1985)

The Volumetric Shale Model

One of the most commonly used equations of this type is the "Simandoux equation", introduced by Simandoux (1963). The Simandoux equation is:

$$\frac{1}{R_t} = \frac{\Phi^m S_w^n}{a R_w} + \frac{V_{sh} S_w}{R_{sh}}$$

where R_t is the formation resistivity, R_w is the formation water resistivity, R_{sh} is the shale resistivity, Φ is the porosity, a , m , and n are the Archie equation constants, V_{sh} is the fraction of shale, and S_w is the water saturation. The Simandoux equation is usually solved as a quadratic, by using $a = 0.81$, $m = 2$, and $n = 2$, which are the Archie equation parameters of the "Ridgefield equation", the Schlumberger variant of the (mathematically) more complex Humble equation to represent typical sandstones. In this specific form, the Simandoux equation becomes:

$$\frac{1}{R_t} = \frac{\Phi^2 S_w^2}{0.81 R_w} + \frac{V_{sh} S_w}{R_{sh}}$$

This is a quadratic equation for water saturation, S_w , and the solution is:

$$S_w = \frac{-b + \sqrt{b^2 - 4ac}}{2a}$$

$$\text{where } a = \Phi^2 / (0.81 R_w)$$

$$b = V_{sh} / R_{sh}$$

$$\text{and } c = -1 / R_t$$

There are many other shaly sandstone equations of the volumetric shale model type and these are reviewed by Worthington (1985). Once the shale indicator has been selected and so V_{sh} determined, the number selected for the value of the shale resistivity, R_{sh} , is the critical parameter in water saturation estimations. Local experience of reservoir saturations and clay characteristics is often the key to success in coaxing these (now) pragmatic equations to produce viable estimates.

The Double Layer Model

The most widely used variant is the "dual-water model" introduced by Clavier et al. (1977). As the name suggests, two kinds of water are postulated: formation water in the granular pore system (both "free water" and capillary-bound water) and clay-bound water, whose salinity and resistivity are different. As before, the resistivity of the formation water is symbolized by R_w , while the clay-bound water resistivity is written as R_b .

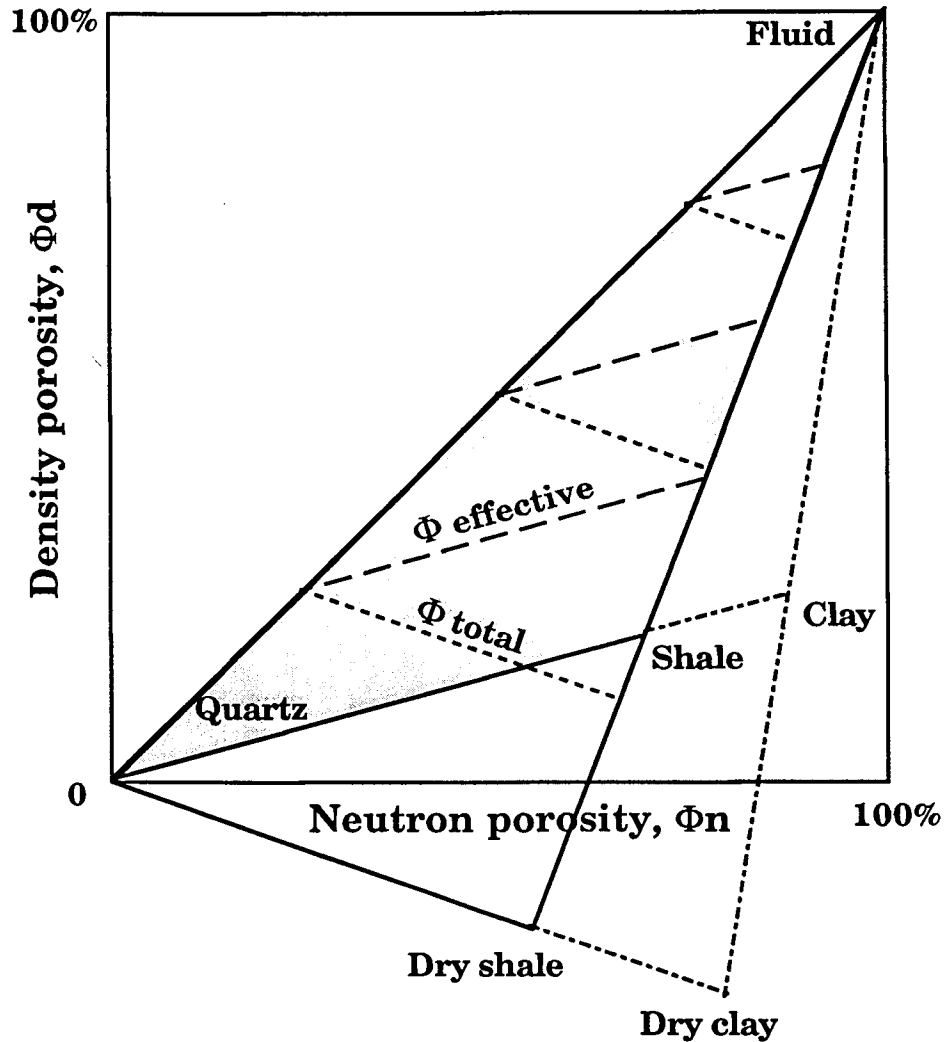
The conventional application of the dual-water model requires the use of the neutron and density porosity logs. In common with other shaly sandstone methods, the volume of shale, V_{sh} , is first calculated and then the effective porosity, Φ_e computed from porosity logs by correcting the apparent porosity for the shale effect. At this point, the dual-water model diverges, because rather than considering the shale to be a single medium, it subdivides the shale into dry matrix and a clay-bound water component. The volume of the clay-bound water added to the effective porosity is the total porosity, Φ_t . For any individual zone, the volume of clay-bound water is determined by the volume of shale multiplied by the "porosity" of the shale, Φ_{tsh} .

The volumetric aspects of the dual-water model may be clarified from the examination of the schematic neutron-density porosity crossplot. Up to this point, the shaly sandstone system has been considered to consist of three components, quartz, fluid, and shale (the gray triangle). The quartz and fluid (mud filtrate) points are calibration points of the log; the shale point is chosen from "representative" shales in the section. In the dual-water model, the shale has a porosity of clay-bound water and its value is a matter of local experience, but is computed from the equation:

$$\Phi_{tsh} = \delta\Phi_{dsh} + (1 - \delta)\Phi_{nsh}$$

where δ takes a value between 0.5 and 1 (Dewan, 1983; Asquith, 1990). The mysterious delta term is simply a pragmatic weighting factor to create a value that seems reasonable as the bound water content of the shale, Φ_{tsh} .

We now have a new composition triangle of quartz, fluid, and "dry shale" where the fluid proportion contours are of total porosity, rather than the effective porosity contained within the triangle quartz-fluid-shale. Ideally, it would be preferable to work within the more fundamental quartz-fluid-clay system, because our aim is to correct for clay mineral conductivity effects within the shaly sandstone. Shale consists of clay minerals and a silt-size fraction of quartz and other (mostly) non-conductive minerals, so that the "wet clay" and "dry clay" points are located on lines that are extrapolations of the shale-quartz lines. Unfortunately, it is highly unusual to see a clay zone in a section and shales are generally what we observe. Even if theoretical corrections are applied to transform shale volumes to hypothetical clay volumes, we have no data on the



Geometry of the dual-water model on a neutron-density porosity crossplot

resistivity of the clay, but are restricted to observations of the resistivity of shale, R_{sh} . In fact, this is all part of a larger problem in that we are using the properties of "external shales" (between the shaly sandstones) to represent "internal shales and clays" whose clay mineralogy and morphology may be radically different. Therefore, the external shale calibrators should be considered as initial model values that are selected to conform as closely to shaly sandstone internal shales as possible, but may be adjusted to give consistent solutions in the shaly sandstone. So, for example, a successful shaly sandstone model should generate values of water saturation close to 100% in fully water-saturated zones. If it does not, then the deviations can be used to fine-tune the model shale parameter values. Examples of this process of "internal calibration" are shown in the following case-study.

Once the total shale porosity value has been established, the total porosity of each zone can be calculated from:

$$\Phi_t = \Phi_e + Vsh\Phi_{tsh}$$

and the clay-bound water saturation computed by:

$$S_b = \frac{Vsh\Phi_{tsh}}{\Phi_t}$$

The bound water resistivity is estimated by an Archie-style equation, by combining the shale resistivity with the shale porosity:

$$R_b = R_{sh}\Phi_{tsh}^2$$

The dual-water model is a quadratic equation that can be solved for the *total* water saturation:

$$S_{wr}^2 - \left[S_b \left(1 - \frac{R_w}{R_b} \right) \right] S_{wr} - \frac{R_w}{(R_t \Phi_t^2)} = 0$$

which can be solved by:

$$S_{wr} = b + \sqrt{b^2 + \frac{R_w}{R_t \Phi_t^2}}$$

where:

$$b = S_b \left(1 - \frac{R_w}{R_b} \right) / 2$$

Finally, the water saturation in the effective pore space can be calculated from:

$$S_w = \frac{(S_{wr} - S_b)}{(1 - S_b)}$$

The results of an initial run of the dual-water model should be evaluated carefully, particularly with respect to zones considered to be fully water-saturated. If the results appear to be at variance with what is known from other information sources, then a revised computation can be made with adjusted model parameter values. If the shale volume, Vsh , estimates are considered to be reasonable, then the parameter values that may need to be adjusted are the resistivity of the shale, Rsh , and the total porosity of the shale, Φ_{tsh} , as revised inputs in a second (or third) run.

Perhaps the best way to gain some practical understanding of the shaly sandstone models is to review their performance in the water saturation analysis of a shaly sandstone. The case study in the following pages uses logging data for a Red Fork Sandstone section in western Oklahoma described by Asquith (1990) in his handbook on log evaluation of shaly sandstones.

THE RED FORK SANDSTONE: A SHALY SANDSTONE CASE-STUDY
Logs and shaly sandstone parameters from Asquith (1990)

In his handbook on shaly sandstone log analysis methods, Asquith (1990) describes the detailed analysis of a single zone (depth 6680 feet) in a section of the Pennsylvanian Red Fork Sandstone. The well is located in western Oklahoma and the Red Fork Sandstone is a fine-grained shaly sandstone, in which shale occurs as dispersed clay. The gamma-ray, neutron and density porosity, and deep induction resistivity logs are shown in the figure. In this manual, we will extend the analysis of the Red Fork Sandstone to the interval in this well between 6620 and 6695 feet depth, and draw on the experience of George Asquith in the selection of shale parameters. Asquith (1990) concluded that the shale at a depth of 6590 feet was representative and recorded these log values for the shale:

Shale resistivity, $R_{sh} = 3$ ohm-m
 Gamma ray = 98 API units
 Shale neutron porosity = 33%
 Shale density porosity = 12%

For the "clean" value of the gamma-ray log, Asquith (1990) chose the minimum at a depth of 6460 feet with a reading of 17 API units.

In this example, there are two alternative methods to estimate shale content, V_{sh} , by using either the gamma ray or the combination of neutron and density porosity logs. Using the gamma-ray log, the transformation is:

$$V_{sh} = \frac{L - C}{S - C} = \frac{L - 17}{98 - 17}$$

Using the density-neutron combination:

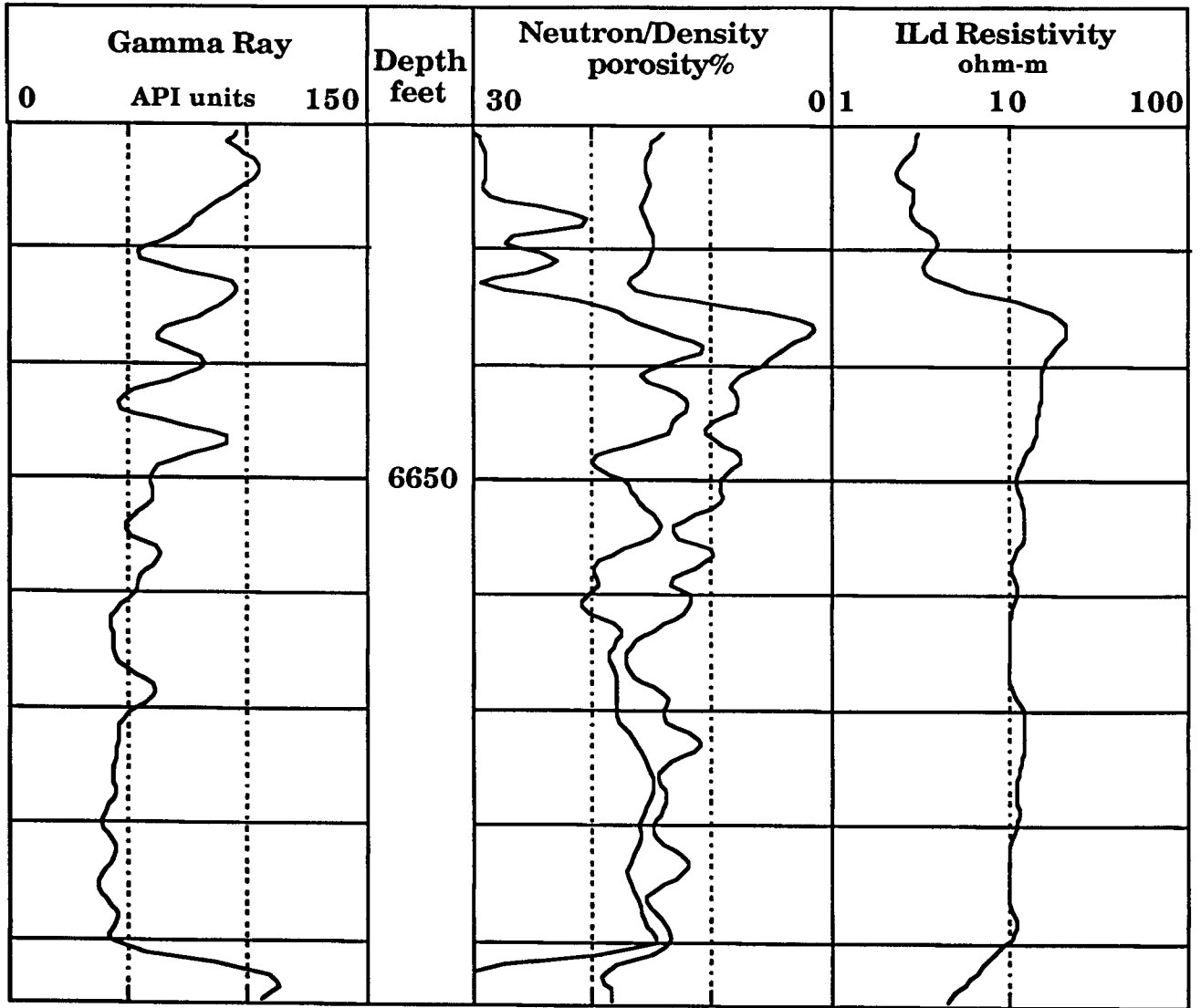
$$V_{sh} = \frac{(\Phi_n - \Phi_d)}{(\Phi_{nsh} - \Phi_{dsh})} = \frac{(\Phi_n - \Phi_d)}{(33 - 12)}$$

The equation to transform neutron-density porosities into shale proportions can be clarified by looking at the neutron-density porosity crossplot, where the shaly sandstone is represented by a compositional triangle with vertices set at quartz, shale, and pore fluid.

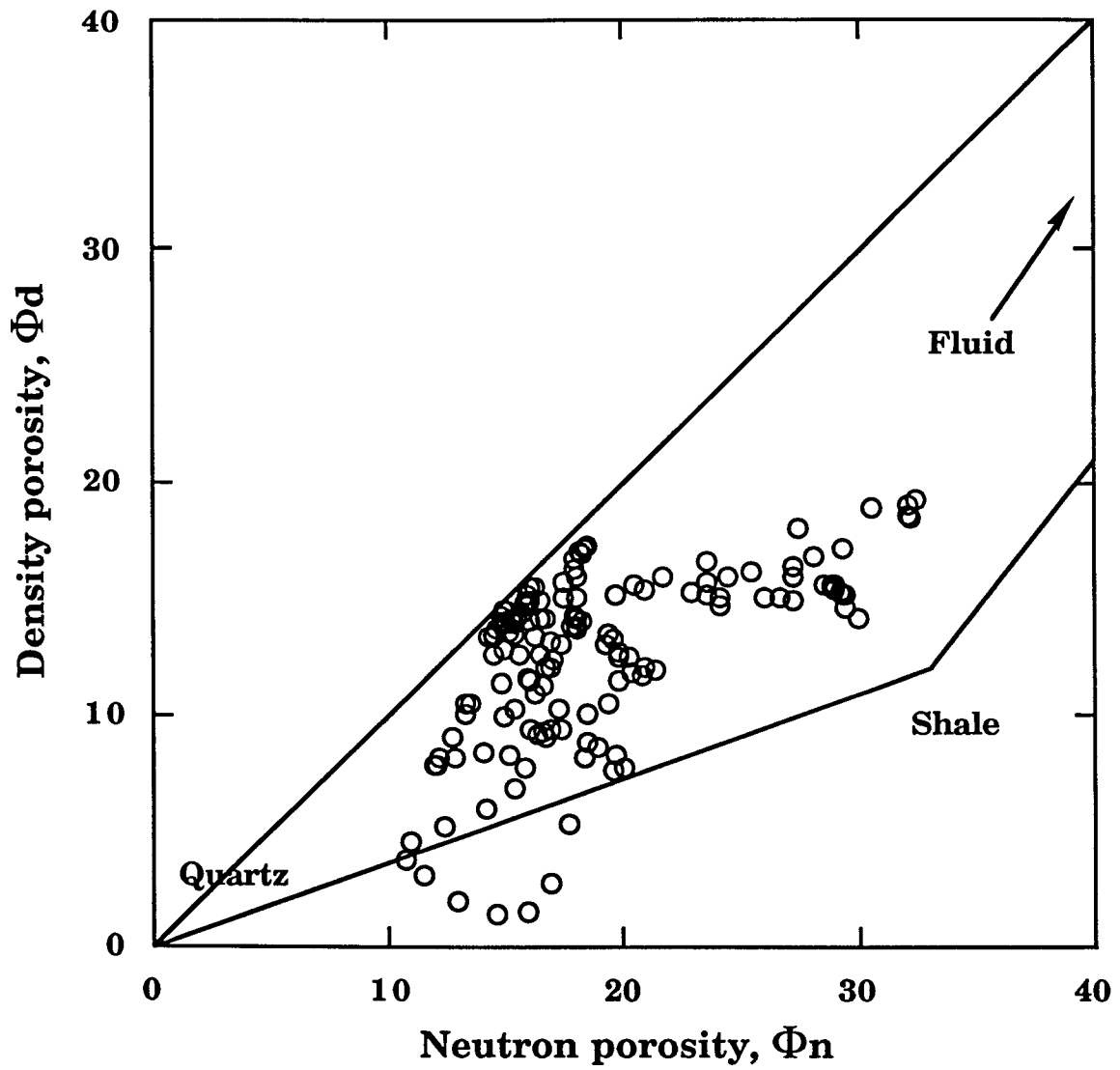
The neutron-density estimate of V_{sh} is consistently lower than the gamma-ray estimate, probably because of additional radioactive sources in the Red Fork Sandstone, such as feldspars and/or micas. The lower estimate is selected as a more reasonable estimate of shale content, in accordance with standard shaly sandstone analysis practice.

The effective porosity is then computed from the neutron and density logs, taking into account the shale content, both in terms of its quantity, V_{sh} , and its properties,

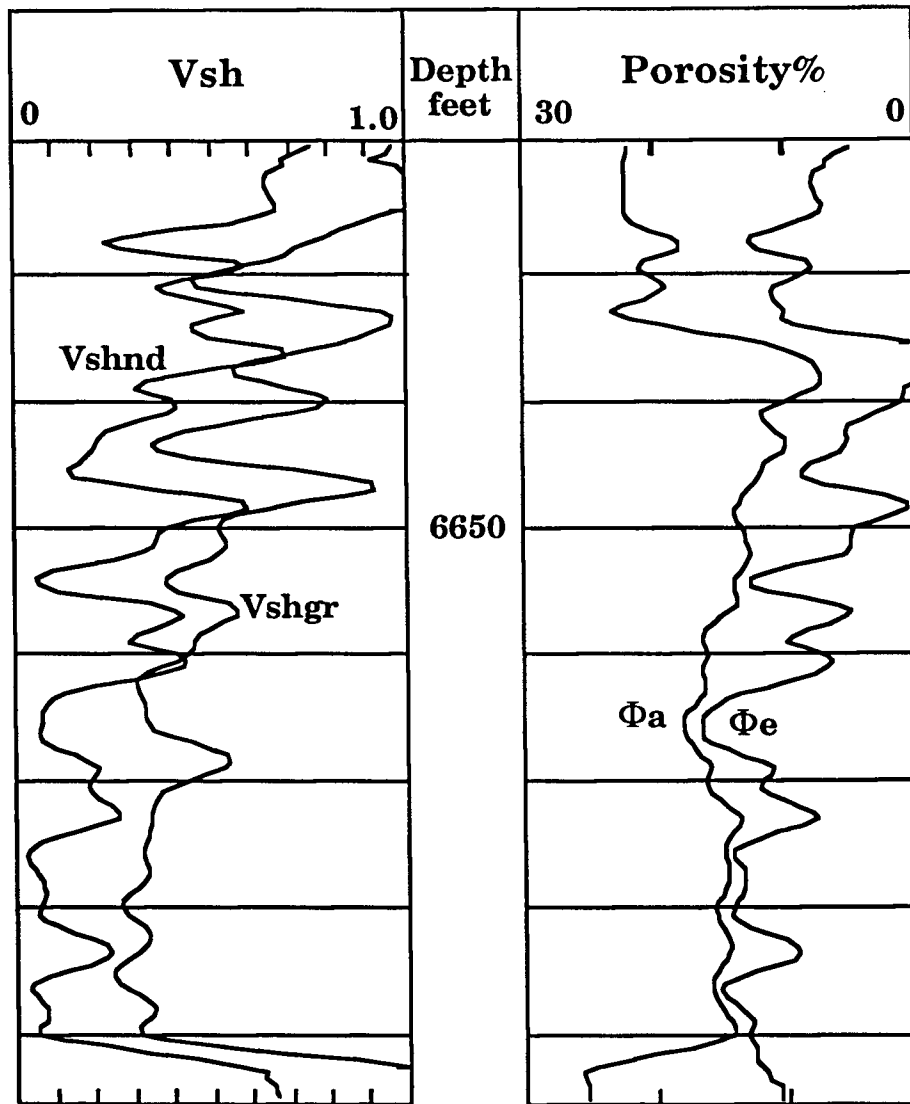
Φ_{nsh} and Φ_{dsh} :
$$\Phi_e = \frac{(\Phi_n + \Phi_d)}{2} - V_{sh} \frac{(\Phi_{nsh} + \Phi_{dsh})}{2}$$



Logs from a section of the Pennsylvanian Red Fork Sandstone in western Oklahoma.
Data from Asquith (1990).



Crossplot of neutron and density porosity logs in the Redk Fork Sandstone well. Log data from Asquith (1990).



The Red Fork Sandstone well: Estimates of shale content from the gamma-ray log (Vshgr) and the neutron-density porosities (Vshnd) recorded as logs in the left track; apparent porosity (Φ_a) that would be computed from uncorrected neutron and density logs compared with effective porosity (Φ_e) computed using a shale correction in the right track.

Now that the effective porosity, Φ_e , has been calculated, the water saturation can be computed. The formation resistivity, R_t , is estimated by the deep induction log. Asquith (1990).

If the Archie equation is applied then the shale effects on the conductivity will be ignored. However, it is useful for comparison purposes as a shaly sandstone baseline, because all the shaly sandstone equations converge on the Archie equation at zero shale levels. The Archie equation estimates will be pessimistic in that conductivity effects of shales are rationalized as water, so that water saturations are overestimated. According to Asquith (1990), the Red Fork Sandstone formation water resistivity at formation temperature is:

$$R_w = 0.05 \text{ ohm-m}$$

and the Ridgefield form of the Archie equation is appropriate, so that:

$$a = 0.81 \quad m = 2 \quad n = 2$$

The Archie equation estimate of water saturation is then given by:

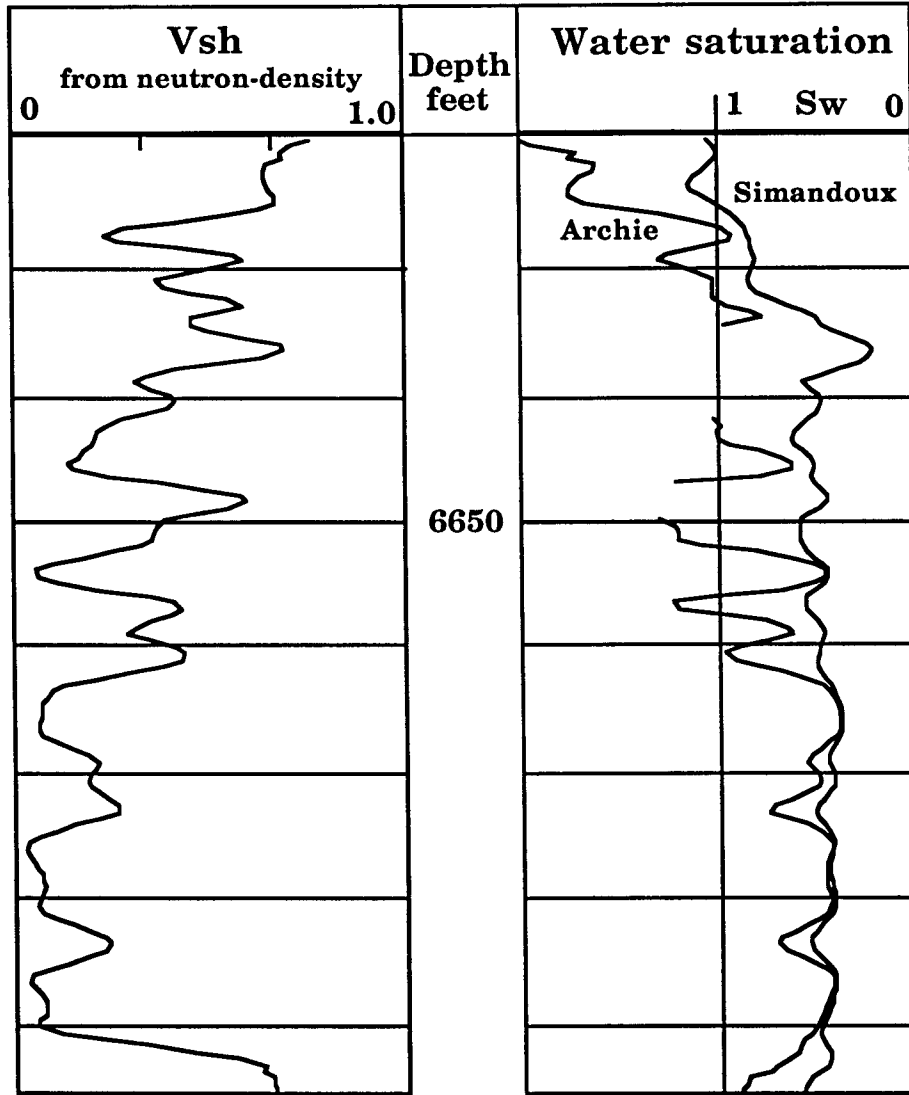
$$S_w = \sqrt{\frac{0.81 R_w}{\Phi^2 R_t}}$$

The Simandoux equation applied to the Red Fork Sandstone is:

$$\frac{1}{R_t} = \frac{\Phi^2 S_w^2}{0.81 R_w} + \frac{V_{sh} S_w}{R_{sh}}$$

Using a shale resistivity (R_{sh}) reading of 3 ohm-m and the fractional volume of shale, V_{sh} , from the neutron and density logs, the Simandoux quadratic equation can be solved for water saturation values.

The water saturation logs from the Archie and Simandoux models are shown for comparison in the following figure. As would be expected, the differences between the two models is small at low shale contents but becomes marked in the more shaly zones. The shaly sandstones at the top of the Red Fork Sandstone section are probably very fine-pored and completely saturated with water. Notice that the Archie equation computes impossibly high water saturations, but that the Simandoux equation predicts water saturations that are close to the expectation of unit value. In fact, intervals that are considered to be totally water-bearing can serve a useful function in shaly sand analysis as internal calibrators. Once a satisfactory method for estimating the volume of shale, V_{sh} , has been accepted, the only other variable specific to the Simandoux equation is the resistivity of the shale, R_{sh} . There will be times when it is difficult to arrive at a "typical" R_{sh} value. Even more commonly, it will be thought that the log properties of the shales *between* the sandstones may not be consistent with shales *within* the sandstones. However, as Worthington (1985) notes "disadvantages can be partially compensated by using R_{sh} as a tuning parameter to improve predictive performance in the water zone in the expectation that better estimates of S_w will thereby be obtained in the hydrocarbon zone." An example of a methodology to achieve this goal is described overleaf.



The Red Fork Sandstone well: Shale proportional volume, Vsh, estimated from the neutron and density logs in the left track; water saturation computed by the Archie equation and the Simandoux equation in the right track.

Spreadsheet software programs such as EXCEL generally contain add-in features that have capabilities beyond routine spreadsheet functions. The EXCEL add-in feature of SOLVER allows the iterative hunt for the best values in "adjustable cells" that cause the value of a "target cell" to be a maximum, a minimum, or close to a given value, as determined by the user.

In this example, we shall propose that the zones between 6620 and 6625 feet are completely water saturated ($S_w=1$). The spreadsheet shows the actual values computed, using the Simandoux equation and parameter values in conjunction with the logs of resistivity (R_t), estimated shale proportion (V_{sh}), and effective porosity (PH_{ie}). The RESID column contains the squared differences between the computed water saturation values and the expected value of 1; the SIGMA cell contains the sum of these squared differences.

We now ask the solver to find the minimum value of SIGMA in the target cell J5, by adjusting the value of R_{sh} contained in cell B11. As shown in the Solver report, the process concludes that a value of 2.67 ohm-m would be the best value for R_{sh} that would give water saturation values as close as possible to unity. This value is so close to the input value of 3 ohm-m selected by Asquith (1990), there is no practical reason to re-run the Simandoux equation over the entire interval. Indeed, this exercise is run more as a demonstration of the procedure. However, in practice, internal calibrations of this kind could be run over multiple horizons in an attempt to improve on parameters deduced from external shales.

| redf.xls | | | | | | | | | | | |
|----------|--|------|---|--------|------|------|-------|-------|---------|-------|---|
| | A | B | C | D | E | F | G | H | I | J | K |
| 1 | RED FORK SANDSTONE (PENNSYLVANIAN), WESTERN OKLAHOMA | | | | | | | | | | |
| 2 | | | | | | | | | | | |
| 3 | Model = Simandoux | | | | | | | | | | |
| 4 | | | | DEPTH | Vsh | RT | PHIe | Sw | RESID | SIGMA | |
| 5 | | | | 6620 | 0.76 | 3.01 | 0.050 | 1.047 | 0.00222 | 0.068 | |
| 6 | PARAMETERS | | | 6620.5 | 0.71 | 2.96 | 0.060 | 1.029 | 0.00087 | | |
| 7 | A | 0.81 | | 6621 | 0.68 | 2.92 | 0.069 | 0.998 | 5E-06 | | |
| 8 | M | 2 | | 6621.5 | 0.69 | 2.86 | 0.068 | 1.015 | 0.00022 | | |
| 9 | N | 2 | | 6622 | 0.65 | 2.66 | 0.076 | 1.034 | 0.00113 | | |
| 10 | RW | 0.05 | | 6622.5 | 0.64 | 2.48 | 0.078 | 1.075 | 0.00567 | | |
| 11 | RSH | 3 | | 6623 | 0.64 | 2.34 | 0.078 | 1.122 | 0.01483 | | |
| 12 | | | | 6623.5 | 0.65 | 2.31 | 0.076 | 1.142 | 0.02009 | | |
| 13 | | | | 6624 | 0.66 | 2.39 | 0.074 | 1.13 | 0.01697 | | |
| 14 | | | | 6624.5 | 0.67 | 2.59 | 0.071 | 1.078 | 0.0061 | | |
| 15 | | | | 6625 | 0.67 | 2.80 | 0.072 | 1.015 | 0.00022 | | |
| 16 | | | | | | | | | | | |
| 17 | | | | | | | | | | | |

$$\text{RESID} = (1 - S_w)^2$$

$$\text{SIGMA} = \sum \text{RESID}$$

| redf.xls | | | |
|------------------------------------|-------|----------------|-------------|
| Microsoft Excel 5.0c Answer Report | | | |
| Worksheet: [REDF.XLS]REDFsim0-5 | | | |
| Report Created: 12/29/97 16:39 | | | |
| Target Cell (Min) | | | |
| Cell | Name | Original Value | Final Value |
| \$J\$5 | SIGMA | 0.068314969 | 0.029267472 |
| Adjustable Cells | | | |
| Cell | Name | Original Value | Final Value |
| \$B\$11 | RSH | 3 | 2.667094626 |
| Constraints | | | |
| NONE | | | |

Internal calibration: An EXCEL Solver solution for Rsh that minimizes the squared differences between water saturations generated by the Simandoux equation and complete water saturations (Sw=1) for the interval 6620-25 feet depth.

In the second part of this case study, we examine the water saturations computed in the Red Fork Sandstone when using the dual-water model. Recall that the dual-water model considers a *total* porosity that consists of the clay-bound water porosity added to the effective porosity in shaly sandstone zones. First, the clay-bound porosity of shales must be specified, and is usually determined by a value of delta in the equation:

$$\Phi_{tsh} = \delta\Phi_{dsh} + (1 - \delta)\Phi_{nsh}$$

Asquith (1990) suggested a value of $\delta = 0.7$ for the Red Fork Sandstone. Because the neutron and density porosities for a representative shale have already been chosen as 33% and 12%, respectively, then the clay-bound water content of the shale, Φ_{tsh} is 18.3%.

Then the total porosity of each zone was computed by:

$$\Phi_t = \Phi_e + Vsh\Phi_{tsh}$$

and the clay-bound water saturation calculated from:

$$S_b = \frac{Vsh\Phi_{tsh}}{\Phi_t}$$

The bound water resistivity is estimated by :

$$R_b = R_{sh}\Phi_{tsh}^2$$

The shale resistivity was already picked to be 3 ohm-m and total shale fractional porosity is 0.183. Therefore, the bound water resistivity, R_b is 0.10 ohm-m.

The dual-water model is then applied to each zone to solve for the *total* water saturation:

$$S_{wt}^2 - \left[S_b \left(1 - \frac{R_w}{R_b} \right) \right] S_{wt} - \frac{R_w}{(R_t \Phi_t^2)} = 0$$

using the standard quadratic equation solution of:

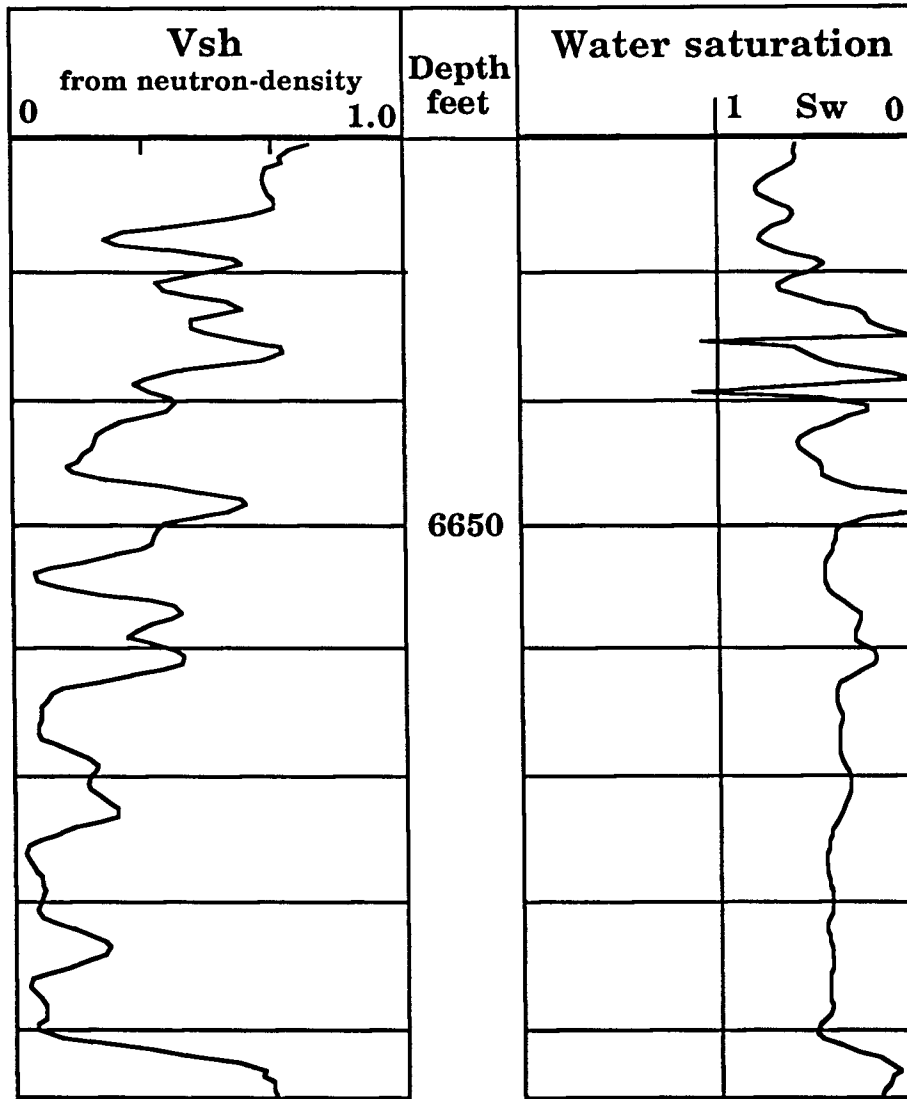
$$S_{wt} = b + \sqrt{b^2 + \frac{R_w}{R_t \Phi_t^2}}$$

where:

$$b = S_b \left(1 - \frac{R_w}{R_b} \right) / 2$$

and then adjusted to the water saturation in the effective pore space using the relationship:

$$S_w = \frac{(S_{wt} - S_b)}{(1 - S_b)}$$



The Red Fork Sandstone well: Shale proportional volume, V_{sh} , estimated from the neutron and density logs in the left track; water saturation computed by the Dual Water Model equation in the right track, using $R_{sh} = 3$ and $\Phi_{tsh} = 0.183$.

Comparison of the water saturation profiles of the Simandoux and Dual-Water models shows the Dual-Water to be more optimistic about hydrocarbon saturation in this case-study. Of course, the result is influenced by the choice of parameter values, and for the dual water model there are two: the resistivity of the shale, R_{sh} , and the clay-bound porosity of the shale, Φ_{tsh} .

In the Simandoux equation solution, we suggested that the zones between 6620 and 6625 feet might be completely water saturated ($S_w=1$). The EXCEL add-in feature of SOLVER was used in an iterative search for the best value of R_{sh} , identified as an "adjustable cell" that would cause the value of a "target cell" of the sum of minimum squared difference between computed water saturations and unity to be a minimum. For the dual-water model, we ask for the best values of both R_{sh} and δ (the weighting factor that determines Φ_{tsh}) to be found that will reach this goal.

The solver attempts find the minimum value of SIGMA in the target cell J5, by adjusting the value of R_{sh} contained in cell B11 and δ in cell B14. As shown in the Solver report, the process concludes that the R_{sh} should be increased to 5.9 and δ adjusted to 0.78. As before, this exercise is run more as a demonstration of the procedure of internal calibration, so that conclusions from this should be tentative at best. However, the approach has a lot to recommend it because although R_{sh} may be misapplied as an external shale resistivity to a clay within the reservoir, where on earth does the value of δ come from? "Experience" can be the only answer, in the absence of laboratory measurements, so the internal calibration approach provides a systematic and consistent method to acquire this experience.

| redf.xls | | | | | | | | | | | | | |
|----------|--|--------|--------|------|------|-------|-------|-------|-------|---------|-------|---|---|
| | A | B | C | D | E | F | G | H | I | J | K | L | M |
| 1 | RED FORK SANDSTONE (PENNSYLVANIAN), WESTERN OKLAHOMA | | | | | | | | | | | | |
| 2 | | | | | | | | | | | | | |
| 3 | Model = Dual water | | | | | | | | | | | | |
| 4 | | | DEPTH | Vsh | RT | PHIe | PHIt | Swt | Swe | RESID | SIGMA | | |
| 5 | | | 6620 | 0.76 | 3.01 | 0.050 | 0.189 | 0.893 | 0.592 | 0.1662 | 1.152 | | |
| 6 | PARAMETERS | | 6620.5 | 0.71 | 2.96 | 0.060 | 0.190 | 0.877 | 0.609 | 0.1531 | | | |
| 7 | A | 1 | 6621 | 0.68 | 2.92 | 0.069 | 0.194 | 0.858 | 0.599 | 0.16065 | | | |
| 8 | M | 2 | 6621.5 | 0.69 | 2.86 | 0.068 | 0.194 | 0.865 | 0.614 | 0.14904 | | | |
| 9 | N | 2 | 6622 | 0.65 | 2.66 | 0.076 | 0.194 | 0.874 | 0.679 | 0.10316 | | | |
| 10 | RW | 0.05 | 6622.5 | 0.64 | 2.48 | 0.078 | 0.195 | 0.894 | 0.733 | 0.07109 | | | |
| 11 | RSH | 3 | 6623 | 0.64 | 2.34 | 0.078 | 0.195 | 0.915 | 0.786 | 0.04576 | | | |
| 12 | PHI _r SH | 0.33 | 6623.5 | 0.65 | 2.31 | 0.076 | 0.195 | 0.924 | 0.806 | 0.03775 | | | |
| 13 | PHI _d SH | 0.12 | 6624 | 0.66 | 2.39 | 0.074 | 0.194 | 0.918 | 0.786 | 0.0459 | | | |
| 14 | delta | 0.7 | 6624.5 | 0.67 | 2.59 | 0.071 | 0.194 | 0.893 | 0.709 | 0.08447 | | | |
| 15 | PHI _t SH | 0.183 | 6625 | 0.67 | 2.80 | 0.072 | 0.194 | 0.865 | 0.632 | 0.13509 | | | |
| 16 | Rb | 0.1005 | | | | | | | | | | | |
| 17 | | | | | | | | | | | | | |

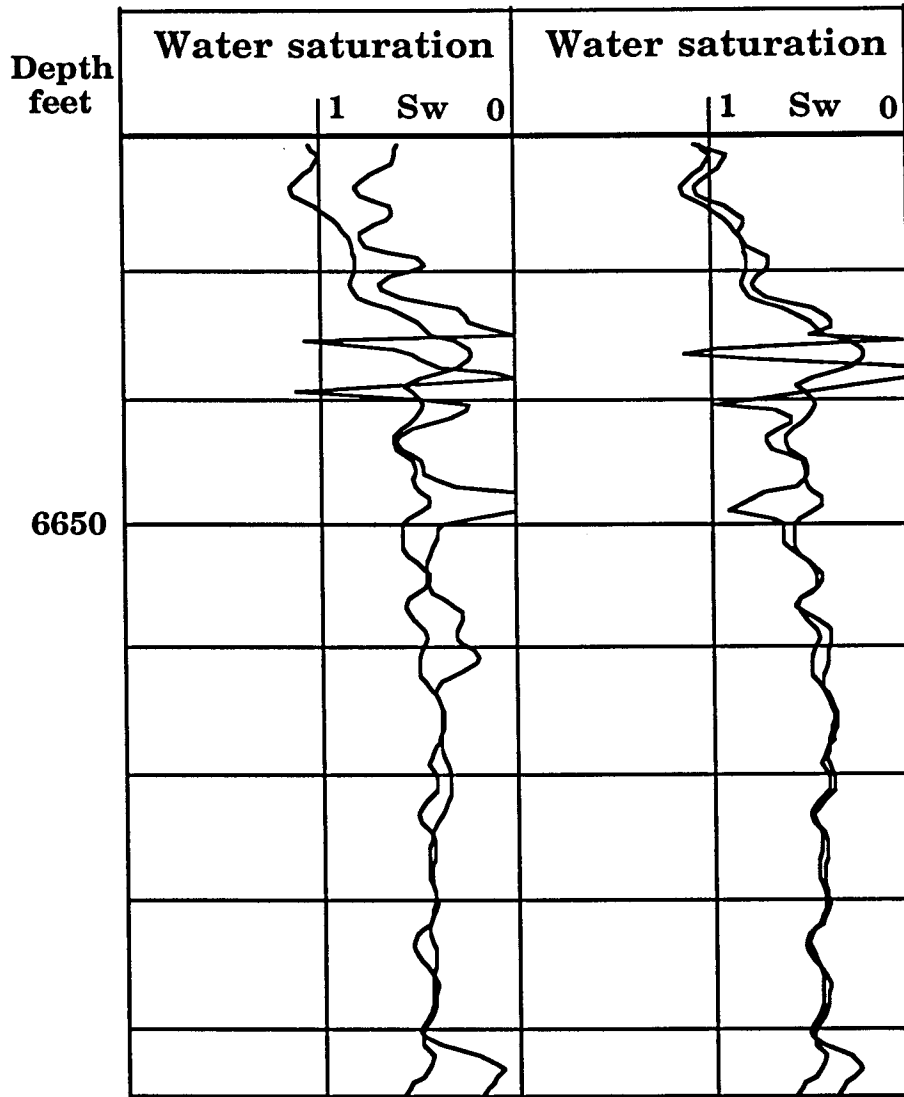
$$\text{RESID} = (1-S_w)^2$$

$$\text{SIGMA} = \sum \text{RESID}$$

| redf.xls | | | |
|---|-------|----------------|-------------|
| Microsoft Excel 5.0c Answer Report | | | |
| Worksheet: [REDF.XLS]REDFtrial | | | |
| Report Created: 12/19/97 12:09 | | | |
| Target Cell (Min) | | | |
| Cell | Name | Original Value | Final Value |
| \$O\$5 | SIGMA | 1.152218212 | 0.037820699 |
| Adjustable Cells | | | |
| Cell | Name | Original Value | Final Value |
| \$B\$11 | RSH | 3 | 5.926660447 |
| \$B\$14 | delta | 0.7 | 0.782115093 |
| Constraints | | | |
| NONE | | | |

Internal calibration: An EXCEL Solver solution for Rsh and δ that minimizes the squared differences between water saturations generated by the Dual-Water equation and complete water saturations ($S_w=1$) for the interval 6620-25 feet depth.

On the following page, the water saturation estimation comparisons are made between the Simandoux and Dual-Water models. Notice that the difference between the two models is substantially diminished following the internal calibration to zones that appear to be completely water-saturated. While nothing is "proved", the similarity gives empirical support to the philosophy expressed in the previous paragraph. It appears that reasonable results can be obtained in shaly sandstone analysis from several possible models, first by selecting shale parameter values from the shales between the shaly sandstone reservoir units and then modifying the values to conform more closely to the clay minerals within the shaly sandstones by calibration on zones considered to be completely water saturated.



The Red Fork Sandstone well: Comparison between water saturation computed by Simandoux model and the Dual Water Model equation, using $R_{sh} = 3$ and $\Phi_{tsh} = 0.183$ (left track), and the Simandoux model and a revised Dual Water Model equation, using $R_{sh} = 5.9$ and $\Phi_{tsh} = 0.166$ (right track).

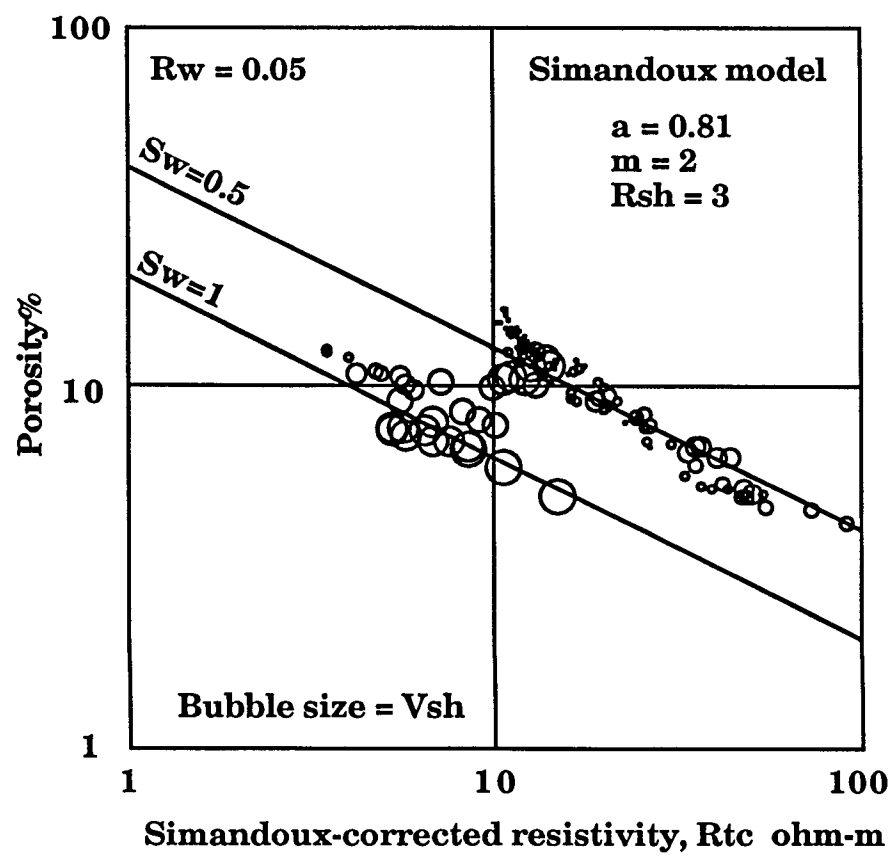
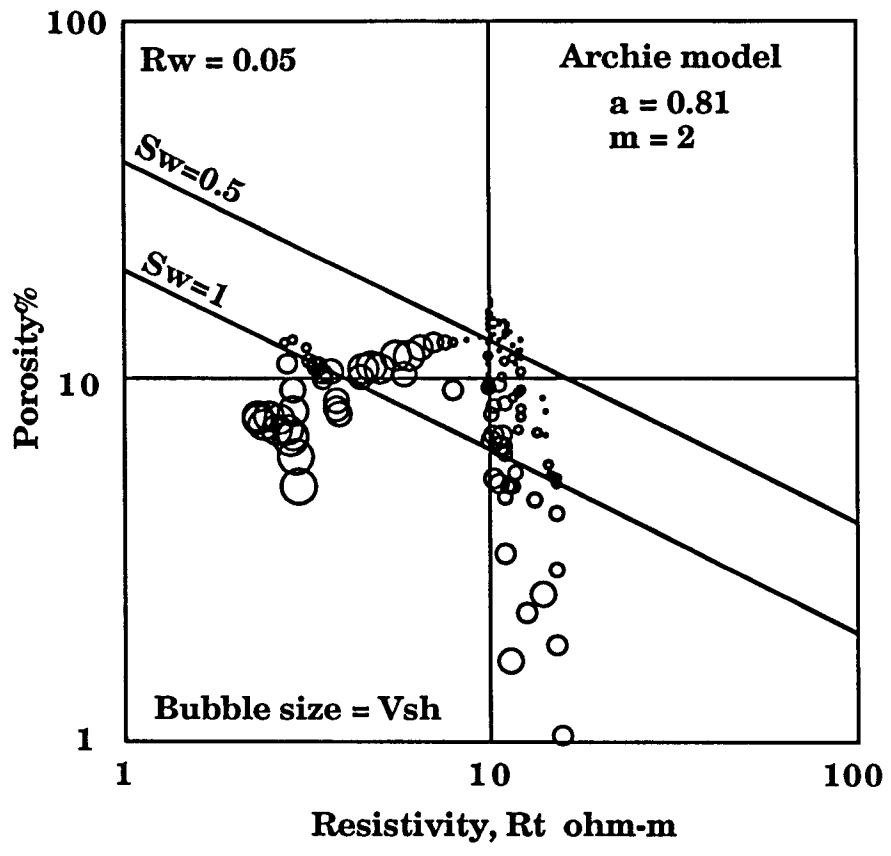
Pickett plots of shaly sandstones

Pickett plots can be made in which the conductivity effects of clays have been eliminated, and so allow petrofacies pattern recognition to be conducted free of disruptive shale effects. This concept was introduced by Aguilera (1990). If the shaly sandstone equation model designed by the user is successful, then a "corrected" resistivity can be computed that predicts the resistivity the rock would have if the clays had no conductivity effects. On the Pickett plot, the crossplot of effective porosity (porosity corrected for shale effects) and shale-corrected resistivity allows the evaluation of patterns and trends in terms of pore-sizes, geometries, fluid saturations, capillary pressure, hydrocarbon column, etc. from a similar perspective to shale-free sections.

A conventional Pickett plot has effective porosity and measured formation resistivity, R_t as its primary axes. On this convention, the conductive "shale effect" on resistivity can be seen, with increases in water saturations, often to impossibly high values as shown in the Red Fork Sandstone Pickett plot. Application of the Simandoux equation (or other shaly sandstone model) produces estimates of water saturation which are (hopefully) close to their true values as fractions of the effective pore space. Data from a shaly sandstone model can be plotted by two alternative methods which lead to the same result. Either the output can be located on the Pickett plot using the porosity and water saturation axes, or a *corrected* formation resistivity can be back-calculated from the water saturations and porosities using the standard Archie equation relationships:

$$R_{tc} = \frac{a * R_w}{\Phi^m * S_w^n}$$

This corrected resistivity is effectively a prediction of the formation resistivity if the clays had no conductivity effects. The modified Pickett plot now has an effective porosity corrected for shale effect and a resistivity corrected for shale conductivity. The result can be seen in the Red Fork Sandstone section where the Simandoux-corrected Pickett plot shows coherent patterns of water-saturated sandstones with high shale contents contrasted with less shaly gas sands.



1964

W-9-167
 STATE Kans COUNTY Pratt MAP NO. 35-295-11W
 OPER Phillips Petroleum Co. Box 287 Gr. Bend, Ks.
 WELL 1 FARM Thompson "J" CLEV. 1809 1811
 PROD. WC PROD. Leben Drlg PROD. Jack Firstenberger
 CO. 4800' Test COMP. 8-10-64 COMP. 9-15-64
 INT. 8-11-64 SPUD. Arbuckle PERD. DSA
 ID 4804

| | | | |
|---|-------|------|-------|
| W.C. S. N.W. of "Abd" Spade Pool (Miss Oil) | Chart | 4584 | 37773 |
| 8" @ 357 w/200 ss (DE Log) | V1 | 4610 | 2799 |
| (DE Spl) | Sp | 2677 | 2854 |
| Hb 36434 | Sp sh | 2691 | 2850 |
| 36575 | Sp sd | 2708 | 2897 |
| Tark 2881 | Arb | 4785 | 2974 |
| How 3127 | | 4804 | 2993 |
| How 3646 | | | |
| Hb 3646 | | | |
| | | | |

OWIWO WILDCAT
 STATE KANSAS 7-2-35 MAP NO. 35-295-11W WFA
 OPER G. N. RUPE SPOT C NE NW WMT
 725 O. W. GARVEY BLDG, WICHITA, KS CO PRATT WF
 WELL I HARDING CLEV. OW 1813 KB FM
 CONTR DAMAC DR LG 1811 ODF, 1809 CGR
 FIELD WC - 1 1/2 MI SE OF SOCIAL PLANS (SP)
 IP D & A
 API 15-151-00496

OLD LOG TOPS:
 TARKIO 2981 - 1004
 HOWARD 3127 - 1114
 HEEBNER 3646 - 1533
 TORONTO 3659 - 1846
 DOUGLAS 3675 - 1862
 LANSING KANSAS CITY 3839 - 2026
 MISS 4346 - 2533
 KINDERHOOK 4423 - 2610
 CHATTANOOGA 4584 - 2771
 VIOLA 4610 - 2799
 SIMPSON 4677

Old Info: Was Phillips Petro, I Thompson "J", SPUD 3-10-64, 5 1/2" 357 w/200, DST 1 (MISS) 4345-69, op 45, Rec 30 Mud w/few oil spks, ISIP 85/30, IFF 9, FFP 19, FSP 105/30
 DST 2 (VI-SP) 4654-88, op 30, Rec 2 gal mud, ISIP 48/30, IFF 19, FFP 29, FSP 38/30
 OTD 4501,
 WAS D & A COMPLETED 9-25-64
 New Info: Re-entered 5-20-75, CO to 3516 PBTD, DST 1 STRD(TARKIO) 2908-26, op 30, no Rec, IFF 34
 DST 2 STRD(TARKIO) 2890-2908, op 30, sl45, Rec 64 Mud, ISIP 604, IFF 40, FFP 40
 DST 3 STRD(ELGIN) 3452-67, op 30, sl45, op 15, sl0, Rec 2 Mud, ISIP 1240, IFF 20, FFP 20, No FSP
 D & A COMPLETED 5-21-75
 Correction: Range was 11E

1975

76
 REPL 1 OWIWO WILDCAT
 STATE KANSAS 3-4-50 MAP NO. 35-295-11W WFA
 OPER RUPE OIL CO. INC. SPOT C NE NW WMT
 BOX 3273, WICHITA, KS CO PRATT WF
 WELL I HARDING CLEV. 1813 KB FM
 CONTR UNION DR LG 1811 ODF, 1809 CGR
 FIELD WC - 1 1/2 MI SE OF SOCIAL PLANS (SP)
 IP D & A
 API 15-151-00496

OLD LOG TOPS:
 LANSING KANSAS CITY 3839 - 2026
 MISS 4346 - 2533
 ARBUCKLE 4785 - 2972
 OTD 4804 - 2991
 TD IN ARBUCKLE 2696 - 883
 NEW LOG TOP INDIAN CAVE 3008 - 1195
 PBTD

1ST OLD INFO: Was Phillips Petroleum, I Thompson "J", SPUD 3-10-64, 5 1/2" 357 w/200, COMPLETED 8-25-64
 OTD 4501, Was D & A, COMPLETED 5-25-75, CO to 3516 PBTD,
 2ND OLD INFO: Re-entered 5-21-75
 3RD INFO: COMPLETED 4-3-76, CC 3008 PBTD, 1 1/2" & 2 3/8 Tbz, 2 2696; Perf 2951 w/150, 100 gal 10" A, 2 3/8 Tbz 7 1/2" A; ATF (IND CV) 2703-09 w/3 SP, 750 gal 7 1/2" A; ATF CP 350
 4 PT. OF 2694 NCFCD, INDIAN CAVE 2703-09 COMPLETED 3-12-76

INDIAN CAVE - HARDING FIELD - DISCOVERY (CONT)

1976

EXERCISE 17:

Well: Phillips Petroleum Thomson #1 (dry hole)

which became

Rupe Oil Harding #1 (discovery)

Producing formation : Indian Cave Sandstone, Admire Group Lr. Permian

Depth : 2696 - 2719 feet subsurface

Lithology : Shaly sandstone

Production : Gas

PROCEDURE

- (1) Take readings from the single "zone" 2703-09 feet (perforation interval) of gamma ray, sonic, and deep induction resistivity logs.
- (2) Compute the shale proportion of the zone from the gamma ray reading and use this value in conjunction with the sonic reading to calculate a porosity which has been corrected for shale content.
- (3) Compute the water saturation of the zone, using the Simandoux equation:

$$\frac{1}{R_t} = \frac{\Phi^2 S_w^2}{0.81 R_w} + \frac{V_{sh} S_w}{R_{sh}}$$

Remember that this is a quadratic equation for water saturation, S_w , and so the solution is given by:

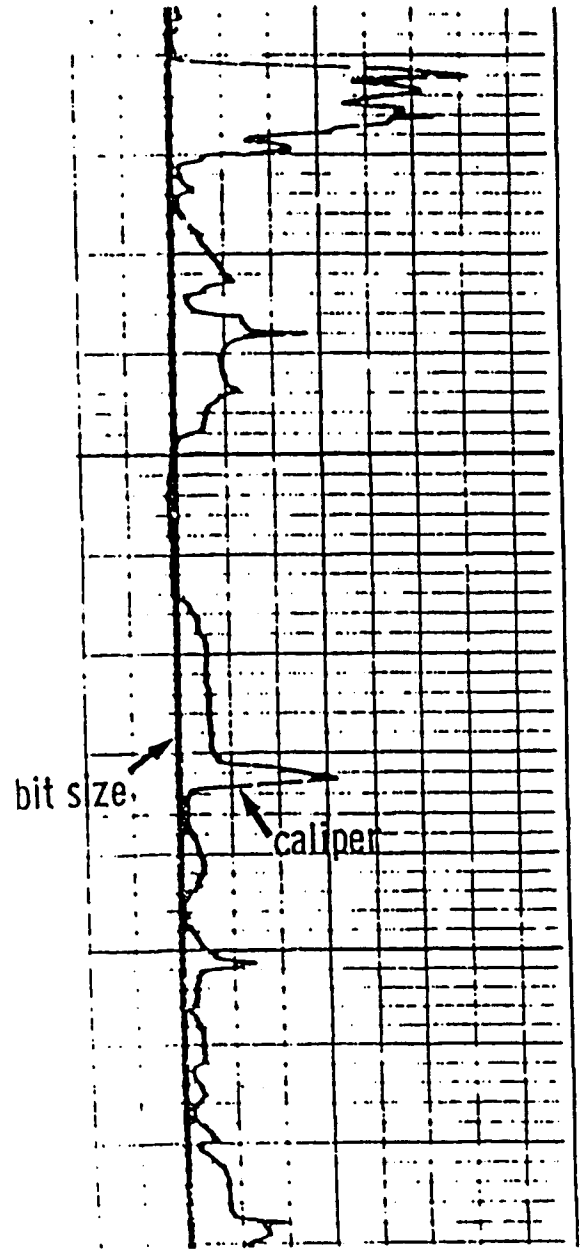
$$S_w = \frac{-b + \sqrt{b^2 - 4ac}}{2a}$$

where $a = \Phi^2 / (0.81 R_w)$

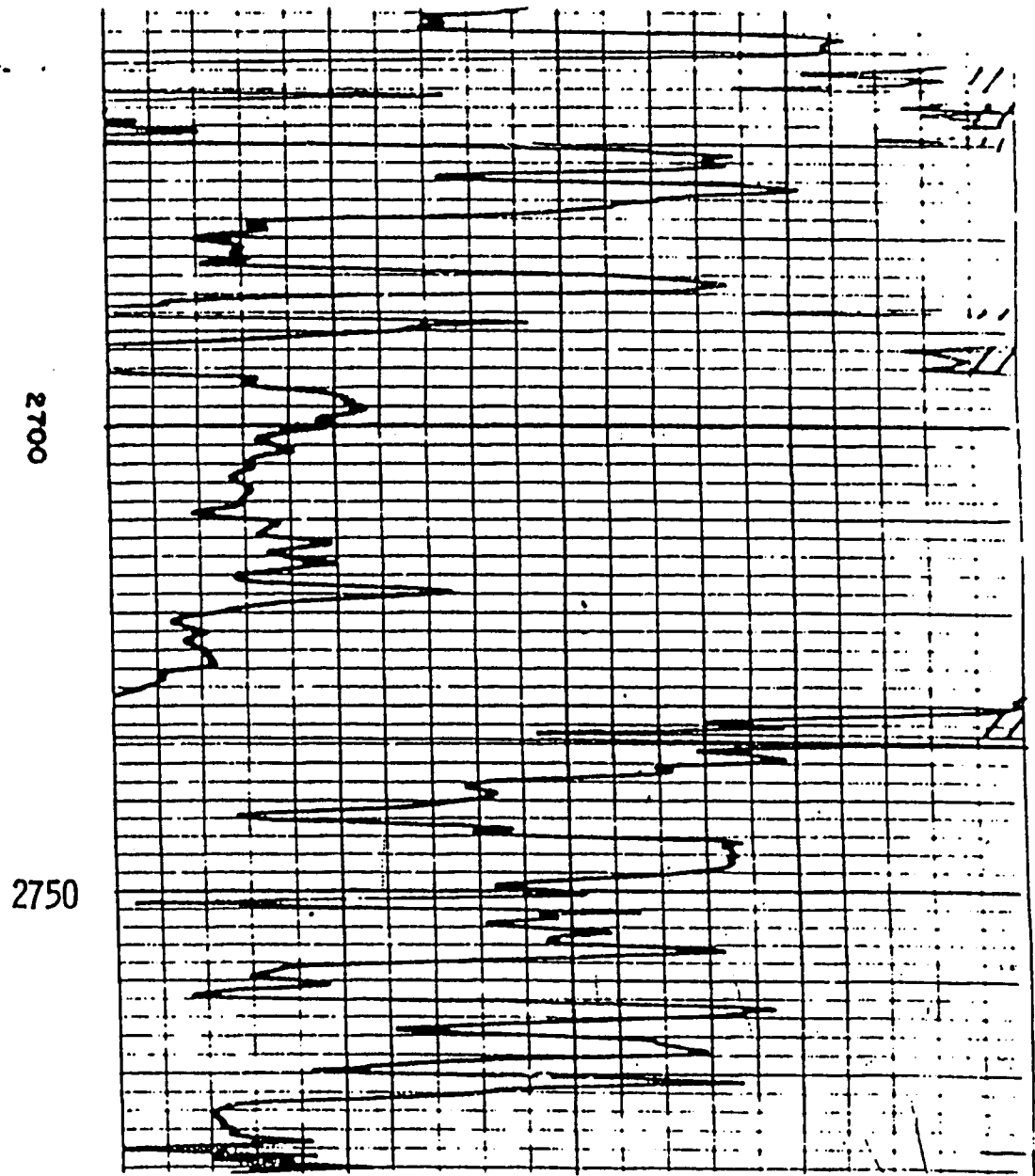
$b = V_{sh} / R_{sh}$

and $c = -1 / R_t$

CALIPER
hole diameter, inches
6" 16"



SONIC microseconds per foot
100 70 40



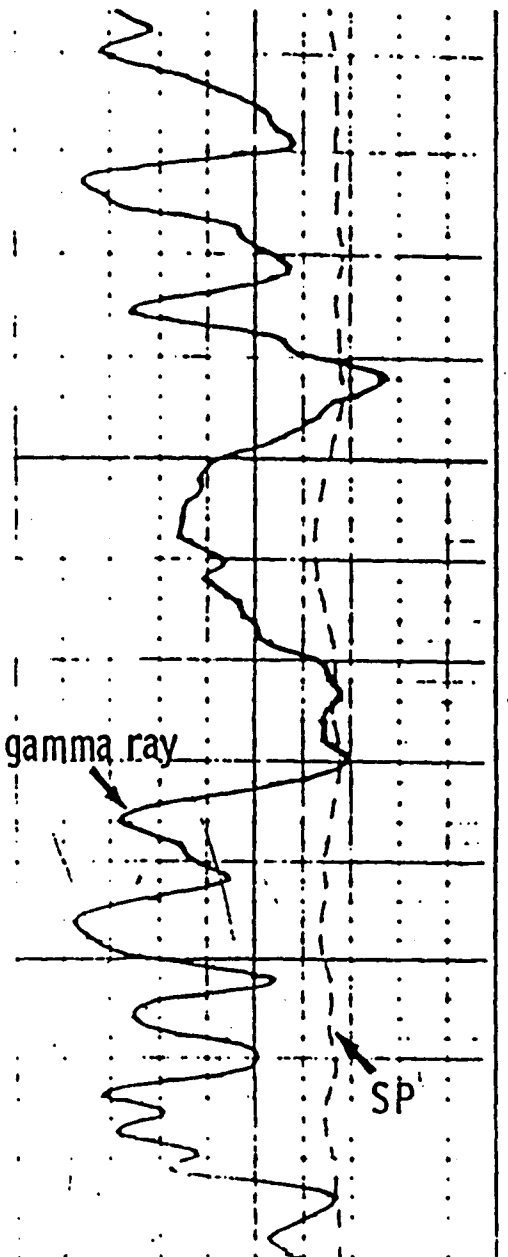
INDIAN CAVE

SP millivolts

- ← 5 → +

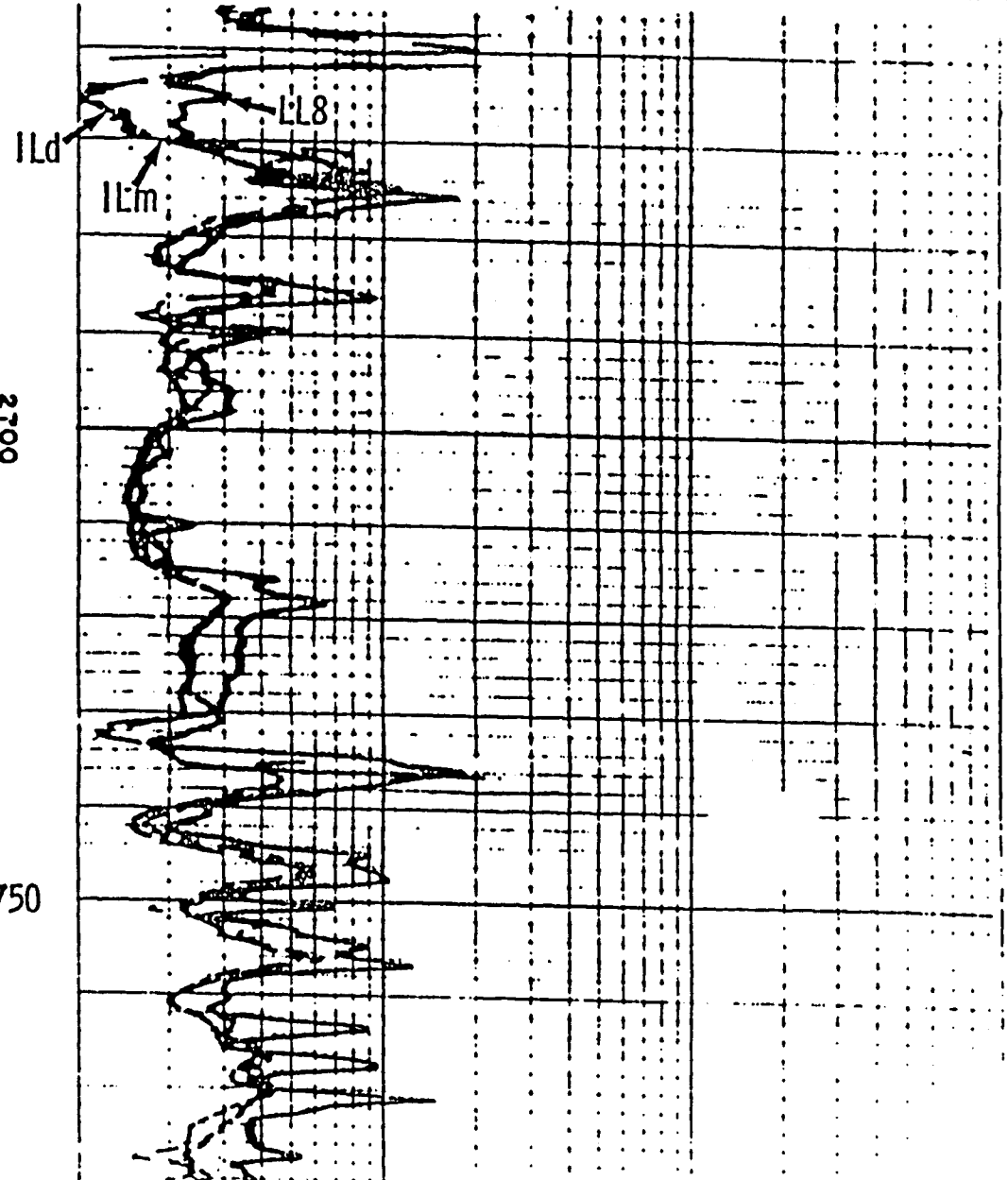
GAMMA RAY API units

0 160



Dual induction - laterolog resistivity ohm-m

1 10 100 1000



INDIAN CAVE

31

2700

2750

Blank

EXERCISE 17: SHALY SANDSTONE ANALYSIS
Indian Cave Sandstone, Kansas

LOG ANALYSIS DATA (deduced from the logs)

GR (clean) = 20 API
GR (shale) = 100 API
 Δt (shale) = 88
 $R_{sh} = 2.5$
 $R_w = 0.03$ @ fmn. temperature

PERFORATION INTERVAL ZONE: 2703 - 09 feet

Log readings of zone:

Gamma ray =
Sonic =
Deep Induction resistivity =

Computations:

V_{sh} =
 ϕ =
 S_w =

The Waxman-Smits shaly sandstone model

Waxman and Smits (1968) formulated the cation-exchange mechanism that causes clay conductivity in shaly sandstones as a double-layer model equation for the solution of water saturation. As with other shaly sandstone models, it was built up from an Archie equation base, but its terms are rooted in the causative physical phenomenon, rather than an implied relationship. By comparison, the older shale-volume models, such as Simandoux, give pragmatic equations, but can be satisfactory if calibrated; other double-layer models were inspired by the theory of the Waxman-Smits formulation, but attempted to adapt the terms to quantities measured on logs, because cation-exchange measurements from core samples are generally quite rare.

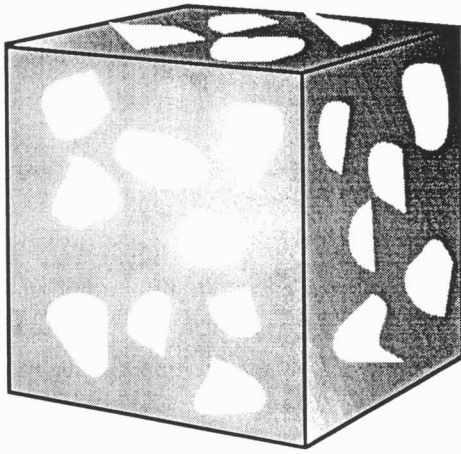
The Waxman-Smits model is based on laboratory observations of shaly sandstones. The resistivity behavior of shaly sandstones that are completely saturated with brine can be understood in terms of an Archie model modified by conductivity caused by cation exchange. Let us consider two hypothetical sandstone cubes which are identical, except that the first is "clean" (no clay minerals with a quartz matrix), while the pore network of the second is coated with clay minerals. The surfaces and edges of the clay minerals have many sites available for the exchange of cations.

If the clean sandstone was flooded with pure water, then both the conductivity of the water and the rock would be effectively zero. If we flushed the pore system with a sequence of successively more conductive brines, the conductivity of the rock would decrease progressively. Crossplotted on a graph of C_w (brine conductivity) and C_o (water-saturated rock conductivity), the points would form a straight line whose slope is the reciprocal of the formation factor, because:

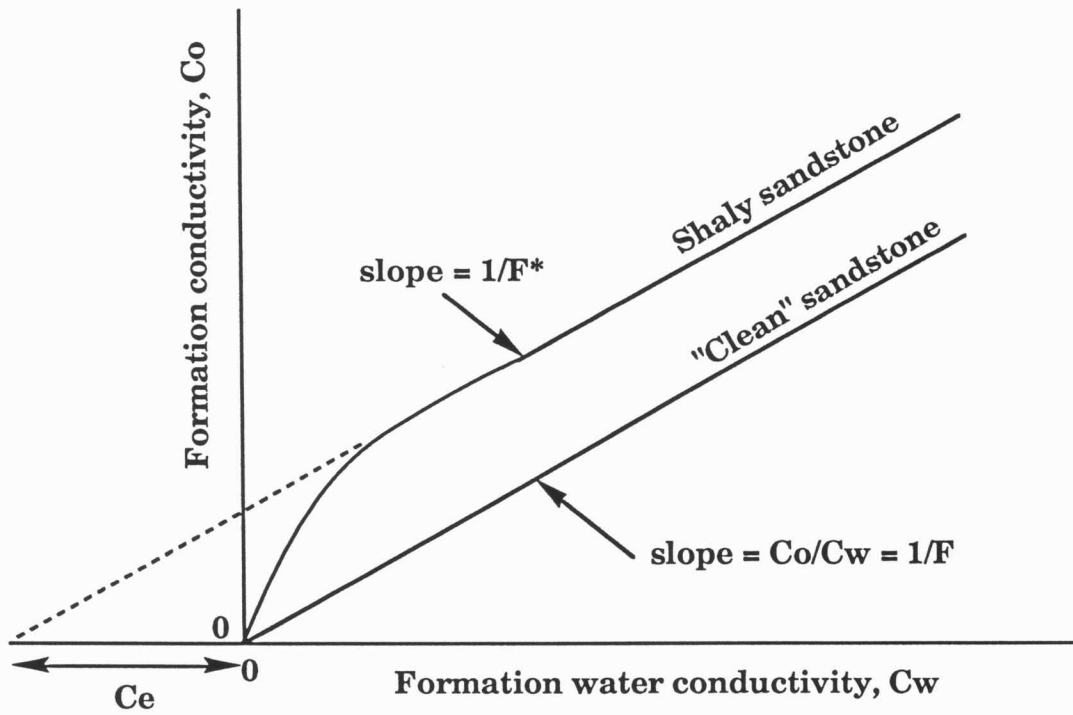
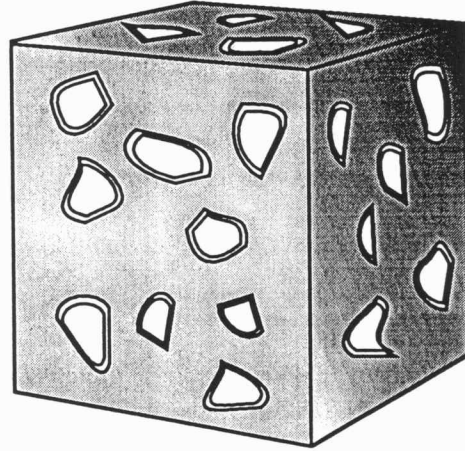
$$\frac{C_o}{C_w} = \frac{R_w}{R_o} = \frac{1}{F} \quad (\text{the first Archie equation})$$

If this procedure was repeated with the corresponding shaly sandstone, the following observations would be made. When the pore fluid was pure water, the conductivity of the rock would be zero, because there are no ions in the water for exchange at clay mineral surfaces, and therefore no conductivity effects. With a small increase in salinity, some (but not all) sites would be activated, and a clay conductivity would be added to the conductivity caused by the ions in the pore space. As the salinity was increased further, there would come a point at which cation-exchange was operating at full capacity, and beyond which no additional clay conduction effects would be added. The conductivity behavior of the water-saturated rock over a range of formation salinities would show a non-linear increase at low brine conductivities that would converge on a linear trend at higher conductivity and approximately parallel to the equivalent clean sandstone line. The slope of the linear segment is, again, equal to the reciprocal of the formation factor, but this is the formation factor of both the open pore space and the clay-bound water and is symbolized as F^* .

"Clean" sandstone



Shaly sandstone



Waxman-Smits model for conductivity in a shaly sandstone that is completely saturated with water

The Waxman-Smiths model equations for water-saturated shaly sandstones are then:

$$C_o = \frac{1}{F^*} (C_w + C_e)$$

where C_e is the conductivity of clay exchange ions

and: $C_e = B \cdot Q_v$

where B is the specific counterion activity (mho/m/equiv/liter) and Q_v is the concentration of exchange cations (meq/ml pore space).

So:

$$C_o = \frac{1}{F^*} (C_w + B \cdot Q_v) \quad \text{and} \quad F^* = \frac{a^*}{\Phi^{m^*}}$$

In the case of a shaly sandstone that is partly saturated with hydrocarbon, the Waxman-Smiths model expands in the equation development that follows. Now:

$$C_t = C_o S_w^{n^*}$$

where C_t is the conductivity of the formation (the reciprocal of R_t) and n^* is the saturation exponent of the shaly sandstone.

So:

$$C_t = S_w^{n^*} \frac{(C_w + B \cdot Q_v)}{F^*} \quad \text{where:} \quad Q_v = \frac{Q}{S_w}$$

The modification of the exchange cations concentration (Q_v) occurs because the hydrocarbon phase concentrates the cations in a smaller volume of pore water.

Written in resistivity (rather than conductivity) terms, the Waxman-Smiths shaly sandstone equation for water saturation becomes:

$$R_t = \frac{F^* R_w}{S_w^{n^*} \left(1 + \frac{B Q_v R_w}{S_w} \right)}$$

The information sources for the parameters to solve the Waxman-Smiths equation are reviewed below:

- Rt: The deep formation reading from the resistivity log.
- F*: The formation factor of the shaly sandstone derived either from measurement or predicted from porosity, based on $F^* = a^* / \Phi^{m^*}$
- Rw: The formation water resistivity measured from a DST or produced water sample, or from an SP log estimation in a clean sandstone, or deduced from resistivity log readings in a contiguous clean sandstone.
- B: B is an index of the mobility of the adsorbed cations on the clay surfaces. B is a function of both temperature and formation water salinity.

Empirical work by Waxman and Thomas (1974) gives the relationship:

$$B = \frac{A}{(1 + X \cdot R_w^{1.23})}$$

where:

$$A = -1.28 + 0.225T - 4.059 \cdot 10^{-4} T^2$$

and: $X = 0.27 + 0.045T$

where T is the formation temperature in degrees centigrade.

Qv: Qv is the concentration of exchange cations measured in meq/ml of pore space. Qv can be calculated from the cation-exchange capacity, CEC, (meq/100 gm of sample) measured on core from:

$$Q_v = \frac{CEC \cdot (1 - \Phi) \cdot \rho_{ma}}{100 \cdot \Phi}$$

When extending laboratory measurements to entire sections, Lavers, Smits, and Van Baaren (1974) proposed the empirical relationship:

$$Q_v = d\Phi^{-e}$$

where d and e are constants to be evaluated from a set of Qv and porosity measurements from core. The form of the equation attempts to relate Qv with the internal surface area of the sandstone estimated by some exponential function of the porosity (dimensionally converting a volume into an area). Use of such an equation allows a prediction of Qv in the subsurface, based on porosity log measurement. Most attempts to relate Qv with some function of Vsh have failed to find a usable relationship.

Characteristics of the Waxman-Smits equation

- (1) In the limiting case of $n^*=2$, the equation is a quadratic expression of Sw. Otherwise the equation is a generalized polynomial that requires an iterative algorithm for solution.
- (2) When no cation-exchangeable clays are present, the equation collapses to the conventional clean sandstone Archie equation.
- (3) The "resistivity distortion" (reduction of Rt from its expected value on the clean sandstone model):
 - (a) increases with increasing hydrocarbon saturation;
 - (b) increases with increasing formation water resistivity.
- (4) This is a model. Assumptions are:
 - (a) parallel conductance for electrolyte and clay-exchange cation components;
 - (b) an exchange-cation mobility that increases to a maximum and constant value with increasing electrolyte concentration;
 - (c) the same geometric conductivity constants apply to both the electrolyte conductivity and the exchange cation conductance.

CLAY MINERALS IN SHALY SANDS: RESERVOIR EFFECTS AND RECOGNITION FROM LOGS

Older shaly sandstone models consider shale only from the point of *morphology* and distinguish between laminar, dispersed, and structural forms of shale component. However, the recognition of clay mineral types within the shale phase has important implications for reservoir performance and management. Illite, chlorite, and smectite both coat pore surfaces and bridge pores and pore-throats, while migrating particles of kaolinite can block pore-throats. As a general trend, permeability is progressively reduced in the sequence: kaolinitic, chloritic, illitic sandstones (Wilson, 1982), which reflects the increasingly adverse effects of discrete particles, pore-lining clays, and pore-bridging clays (Neashan, 1977). Smectite is also extremely sensitive to fresh water which causes swelling, while chlorite is highly acid-sensitive, with the formation of iron hydroxide as a precipitate to clog pore throats. As a result, knowledge of clays is important both in primary production, as well as secondary recovery involving water flooding or acid treatment.

The effects of clay mineral species on different types of logs are summarized below and can help in their recognition:

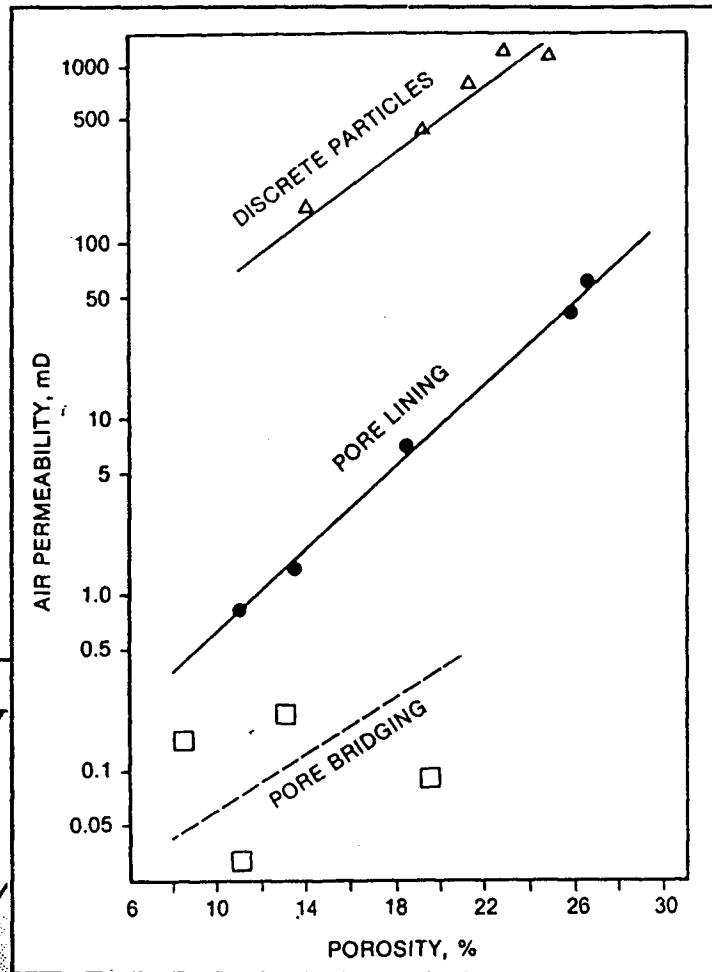
Gamma-ray log

Clay minerals generally have thorium absorbed at their surfaces, may contain potassium, and may be associated with uranium fixed by either organic material or phosphatic minerals. Both illite and smectite cause higher readings on gamma-ray logs because of thorium and potassium contents, but the effects of kaolinite and chlorite are variable. There are many instances of kaolinitic and chloritic sandstones that are difficult to distinguish from clay-free sandstones on the gamma-ray log and has earned them the name of the "invisible clays" with some log analysts. However, kaolinite can be quite radioactive and its radioactivity seems to be controlled by how it was formed. If created by authigenic alteration within sandstones, it will often have low thorium and potassium content. If the kaolinite results from extensive leaching in a soil, then it may have moderate to high thorium contents and therefore be significantly radioactive.

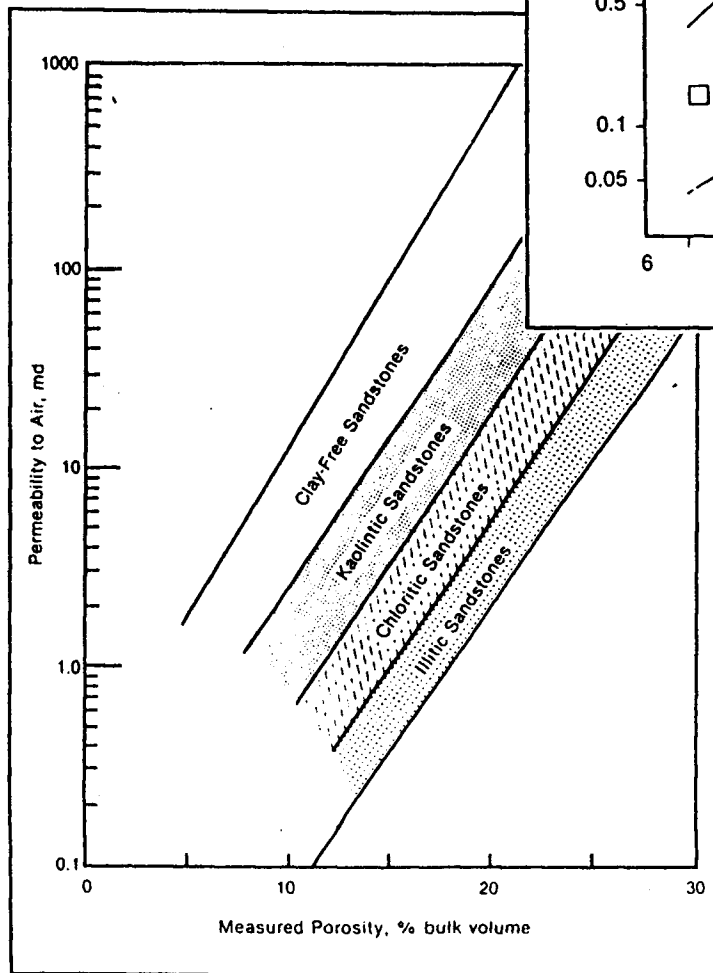
Resistivity log

Clay minerals have cation-exchange capacity (CEC) caused by charge at the mineral surfaces. Smectite has the highest CEC, followed by illite and chlorite, with kaolinite having the lowest CEC. However, because the effect is a surface area phenomenon, actual values will vary with particle size, so that CEC increases with finer-grade particles.

INFLUENCE OF CLAY MINERALS / CLAY MORPHOLOGIES ON POROSITY - PERMEABILITY RELATIONSHIPS IN SANDSTONES



(Neashan, 1977)



(Wilson, 1982)

Photoelectric absorption (Pe)

Density tools now make an additional measurement of the absorption of low-energy gamma rays by the photoelectric effect. The photoelectric factor (Pe) is measured in barns per electron and is a direct function of the aggregate atomic number of the formation. In clastic lithologies, the atomic number for clay aluminosilicates such as kaolinite is very similar to quartz, so that they are difficult to differentiate. However, the substitution of iron within the clay mineral lattice is a major cause of photoelectric factor variation in logs of sandstone shale sequences (Ellis, 1987). Consequently, illitic shales show higher Pe values, with smectite shales intermediate between illite and kaolinite, while iron-bearing chlorites may generate very high Pe values. The exact numbers will depend on the amount of substitution by iron (or other elements with higher atomic number).

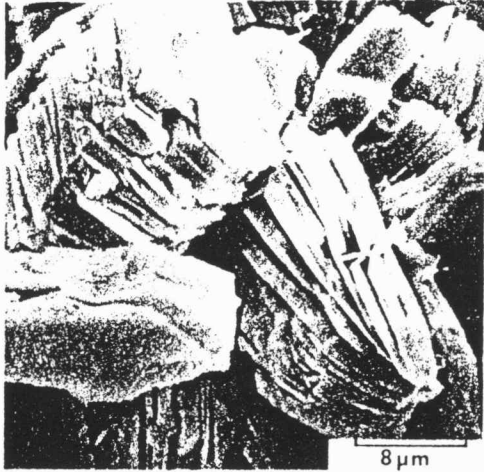
Neutron and density logs

Ellis (1987) pointed out a fundamental distinction between the clay minerals, in terms of their hydroxyl content. Kaolinite and chlorite have eight hydroxyls; illite and smectite have four hydroxyls in their lattice structure. The effects of the hydroxyl content can be seen when comparing the density and epithermal neutron logs when they are both calibrated to a sandstone porosity scale. The epithermal neutron would read about 40 porosity units higher than the density log for either pure kaolinite or chlorite, and about 10 porosity units higher for either pure smectite or illite.

Geochemical logs

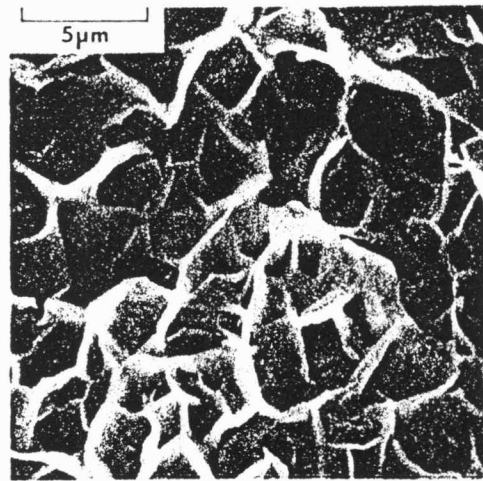
Geochemical logging now makes direct estimates of aluminum by delayed neutron activation, and calcium, silicon, iron, titanium, sulfur, and gadolinium by neutron absorption, in addition to potassium, thorium, and uranium measurements from the natural gamma-ray spectrum. Equations that link elements to minerals have been applied in computational models to analyze the compositions of sedimentary sequences. A number of studies have been made to compare processed estimates of clay mineral types and their quantities with laboratory measurements from core (e.g. Herron, 1986).

LITTLE SHOP OF HORRORS: CLAY MINERALS & THEIR ROLE IN FORMATION DAMAGE



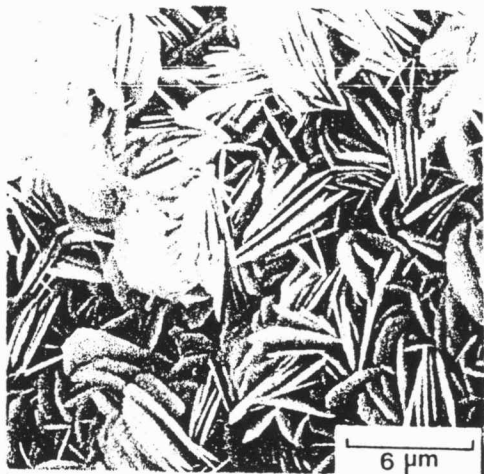
KAOLINITE

patchy discrete particles
Migration of fines which
can block pore throats



SMECTITE

pore - lining / bridging
Highly sensitive to fresh
water, resulting in clay
swelling and microporosity



CHLORITE

pore - lining / bridging
Very acid - sensitive, with
production of iron hydroxide
precipitate to fill pore throats



ILLITE

Pore - lining / bridging
Microporosity formation,
some migration of fines

SEM photos by Syed Ali in Bigelow (1985)

Blank